Inorganic Chemistry

pubs.acs.org/IC

Article

Catalytic Approach toward Chiral P,N-Chelate Complexes Utilizing the Asymmetric Hydrophosphination Protocol

Dávid Katona, Yunpeng Lu, Yongxin Li, Sumod A. Pullarkat,* and Pak-Hing Leung*

Cite This: https://dx.doi.org/10.1021/acs.inorgchem.9b03549

Read Online

ACCESS | Metrics & More | Article Recommendations | Supporting Information

ABSTRACT: A synthetic procedure for obtaining a chiral P,N ligand was developed by exploiting the versatility of the asymmetric hydrophosphination protocol catalyzed by a phospha-palladacycle complex. The addition of the synthesized ligand to various metal sources led to the generation of chiral and enantioenriched chelate complexes, which can be useful prototypes for catalyst design in the future. The resulting coordination compounds were comprehensively characterized by solid-state (X-ray crystallography) and solution-based (one- and two-dimensional NMR spectroscopy) techniques and natural bond orbital (density functional theory) analysis to determine their structural and key electronic features.

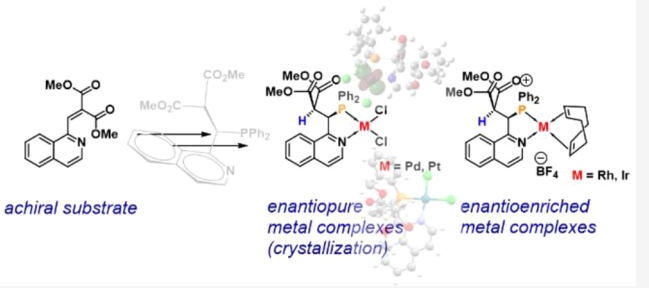

INTRODUCTION

Bidentate ligands and their stereochemical properties play a crucial role in both asymmetric and nonasymmetric transition-metal-mediated catalysis.[1] Diphosphines, as bidentate ligands, have been widely utilized in asymmetric synthesis, e.g., hydroformylation, asymmetric hydrogenation, allylic substitution, and hydrosilylation, because of their proven track record in providing high selectivity.[2] Apart from diphosphines, which remain the most popular class of bidentates used in catalysis, heterobidentate ligands, such as P,N ligands, also have played a significant and emerging role in transition-metal catalysis.[3] They indeed have a proven record in several key transformations such as asymmetric allylic alkylation (employing H_8-MAP or QUINAP),[4] isomerization[5] and asymmetric hydrogenation of allylic alcohols,[6] enantioselective hydroboration,[3b,7] and even in the asymmetric Heck reaction.[8]

In the case of BINAP[9] and QUINAP[10] (Figure 1), the key to their efficiency lies in the rigid and predetermined spatial arrangement that they provide around a certain metal center upon coordination. This kind of steric block has been utilized in numerous cases where chiral induction needed to be efficiently conveyed, including in the chemistry of chiral palladacycles[11] (Figure 2). Because these cyclopalladated compounds play an important role in several asymmetric transformations including Diels–Alder cycloadditions[12] and, more recently, in hydrophosphinations,[11d,13] our aim was to design a new P,N bidentate system based on the structure of (*R*)-**2**[14] (Figure 2). Such a modification will then allow us, from the point of catalyst design, to vary the metal center and access and exploit a broader scale of oxidation states. It is envisaged that by switching the coordinating moiety located in the aryl backbone from an sp^2 carbon atom to a sp^2 nitrogen atom, the electronic properties at the metal center will be altered, and this can enhance its reactivity toward oxidative addition.[3b,15]

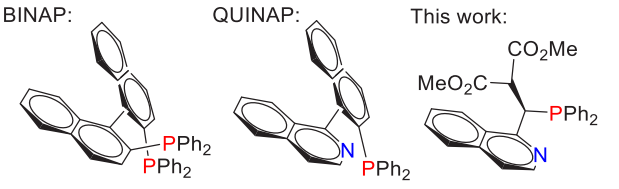

Figure 1. Chiral ligands for asymmetric catalysis including the new P,N ligand synthesized by us.

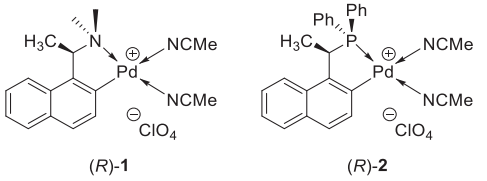

Figure 2. Chiral palladacycles: versatile tools in asymmetric synthetic protocols.

Received: December 5, 2019

However, the synthesis of such chiral heterobidentate P,N ligands traditionally requires tedious manipulations, including multiple steps and resolution protocols that can adversely impact the atom economy.[3b,10a] Although novel syntheses of QUINAP have been reported by both Stoltz et al.[16] and Lassaletta et al.[17] by using dynamic kinetic resolution and dynamic kinetic asymmetric transformation, respectively, those syntheses use racemic mixtures as starting materials.

In our case, however, by utilizing the asymmetric hydrophosphination reaction, the synthetic route produces an enantioenriched P,N ligand from a truly achiral substrate. Having obtained the enantioenriched P,N phosphine ligand, we were able to generate a class of unreported complexes incorporating the new P,N ligand system, such as enantiopure dichloropalladium and -platinum complexes, and enantioenriched rhodium and iridium cyclooctadiene complexes. The investigation of the structural, steric, and electronic behavior of these complexes by one- and two-dimensional NMR spectroscopy and X-ray crystallography was also undertaken. The experimental results were supported by using density functional theory (DFT) methods, such as structure optimization and natural bond orbital (NBO) analysis, conducted to provide insight into the π acidity of the P,N ligand. The collected data on these model compounds can be useful for the design and application of these complexes and their derivatives in catalytic protocols.

RESULTS AND DISCUSSION

Synthetic Scheme. Because we intended to apply asymmetric hydrophosphination in a synthetic pathway to generate the P,N ligand motif, it was necessary to synthesize the activated olefin, which already incorporated an sp^2 nitrogen atom. The synthetic challenge, however, in attempting this is that typically small bite-angle P,N heterobidentate ligands can themselves disrupt the catalytic cycle of the palladium-catalyzed asymmetric hydrophosphination reaction by forming a chelate with the catalyst, thus disrupting the process by which the phosphine substrate can be displaced from the metal center by the nucleophilic diphenylphosphine moiety present in the reaction system.[11a,d,13] To design a suitable substrate to test the performance of various known hydrophosphination catalysts and to surmount the aforementioned challenge, isoquinoline **3** was functionalized in the first position by a selective radical formylation reported by Minisci et al. in 1986,[18] which led to a cyclic acetal **3a** (1,3,5-trioxane derivative). After deprotection,[19] the desired carbaldehyde **4** was isolated (Scheme 1).

Scheme 1. Synthetic Scheme for Functionalizing Isoquinoline

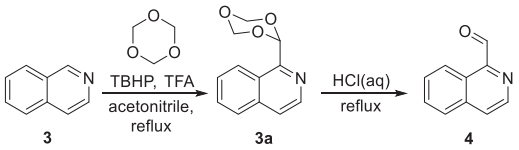

The aldehyde **4** was then successfully reacted with dialkyl and diaralkyl malonates in condensation reactions,[20] which provided the activated olefin substrates (Figure 3).

It has been seen from previous studies conducted by us that the presence of two −COOR moieties is essential to provide the optimum activation, which allows the subsequently

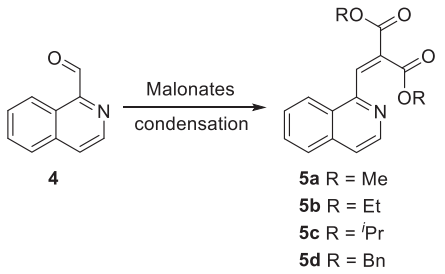

Figure 3. Synthesis of the activated olefin for asymmetric hydrophosphination.

planned catalytic hydrophosphination reaction to proceed smoothly.[21] The hydrophosphination reaction was optimized by using the dimethyl malonate derivative **5a** as a substrate, while both the (*S*)-**2** and (*R*,*R*)-**7** catalysts were employed[21b,22] (Table 1). The resulting phosphine was treated with sulfur upon completion of the reaction to obtain phosphine sulfides, which could be handled easily to carry out high-performance liquid chromatography (HPLC) and other measurements. As aforementioned, based on our previous experience, we expected that the phosphapalladacycle catalyst (*S*)-**2** was not suitable for the planned hydrophosphination of this substrate because of the intramolecular pathway that the Michael-addition process is known to undergo in this class of catalysts. The presence of the aromatic nitrogen atom, in conjunction in **5a** along with the newly introduced phosphine, can cause catalyst poisoning at the palladium center via a strong P,N chelation upon product formation.[11d,23] We envisaged that for this particular substrate the pincer-type metallacycle complex (*R*,*R*)-**7** would be a more suitable catalyst because it promotes the catalytic hydrophosphination protocol in an intermolecular fashion, thus precluding the chance of product chelation and subsequent catalyst poisoning.[24] However, to our surprise, the (*S*)-**2** complex indeed showed a good catalytic performance, while the pincer type (*R*,*R*)-**7** catalyst did not prove to be successful in delivering either significant enantiomeric excess (ee) or higher yield. The progress of the hydrophosphination reactions was monitored by $^{31}P\{^{1}H\}$ NMR spectroscopy.

It was revealed during the optimization studies that the optimum condition was when triethylamine (TEA) was used as a base in dichloromethane (DCM) at −80 °C while using (*S*)-**2** as the catalyst (entry 8). In this instance, the hydrophosphination reaction proceeded smoothly, providing 82% ee of the expected product with 65% yield. By close monitoring of the yield and ee of the reaction, it was observed that the conversion reached its maximum after 72 h. Increasing the reaction temperature could not assist in the completion of the reaction, but it caused proportionally lower ee in each case (entries 9 and 10). We also concluded that the selectivity of the reaction is sensitive to the concentration of the catalyst (entry 11).

During screening of the base, we found that the use of 1.0 equiv of TEA was necessary for catalysis to take place: The reaction could not start either in the absence of a base or by using a weaker base or a lower base loading (entries 13−15). Another observation was that the application of a stronger base, e.g., 1,8-diazabicyclo[5.4.0]undec-7-ene (DBU) led to a racemic product mixture, although the reaction proceeded to completion (entry 16). Another interesting fact that was observed during the optimization studies was that the reaction

https://dx.doi.org/10.1021/acs.inorgchem.9b03549
Inorg. Chem. XXXX, XXX, XXX−XXX

Table 1. Optimization and Application of the Hydrophosphination of Activated Olefins 5a−5d

entry	R	catalyst[a]	base[c]	solvent	T/°C	t/h	yield/%[e]	ee/%
1	Me	$Pd(OAc)_2$		DCM	25	2	66	0
2	Me	(*R*,*R*)-**7**		DCM	25	18	57	0
3	Me	(*R*,*R*)-**7**		DCM	−40	24	50	0
4	Me	(*S*)-**2**	TEA	THF	−80	55	76	1.7
5	Me	(*S*)-**2**	TEA	toluene	−80	17	69	1.6
6	Me	(*S*)-**2**	TEA	MeOH	−80	22	44	13
7	Me	(*S*)-**2**	TEA	acetone	−80	72	86	44
8	Me	(*S*)-**2**	TEA	DCM	−80	72	65	82
9	Me	(*S*)-**2**	TEA	DCM	−40	72	99	25
10	Me	(*S*)-**2**	TEA	DCM	−60	72	72	49
11[b]	Me	(*S*)-**2**	TEA	DCM	−80	66	75	73
12	Me	(*R*)-**2**	TEA	DCM	−80	72	60	55
13	Me	(*S*)-**2**		DCM	−80			
14[d]	Me	(*S*)-**2**	NaOAc	DCM	−80			
15[d]	Me	(*S*)-**2**	TEA	DCM	−80			
16	Me	(*S*)-**2**	DBU	DCM	−80	72	60	0
17	Et	(*S*)-**2**	TEA	DCM	−80	264	58	25
18	^{i}Pr	(*S*)-**2**	TEA	DCM	−80	216	NA	NA
19	Bn	(*S*)-**2**	TEA	DCM	−80	288	64	61

[a]5 mol % catalyst was loaded, unless otherwise noted. [b]10 mol % catalyst was loaded. [c]1 equiv of base was used unless otherwise noted. [d]10 mol % base was used. [e]Isolated yields.

can indeed proceed without the metal at room temperature (RT) with the use of 1.0 equiv of TEA.

However, the conversion was significantly slower than that achieved by employing the palladium catalyst, and, as expected, no stereoselectivity was achieved. This occurrence of a background nonmetal-catalyzed hydrophosphination has been observed by us previously for activated ligands and necessitates conduction of the reaction at low temperature in order for the metal-catalyzed pathway to dominate and provide enantioselectivity.

Given that the formed P,N ligand bears an acidic proton on the carbon atom adjacent to the chiral center, our concern was that the acid−base equilibrium could occur in the basic medium, and this could potentially lead to side reactions, which would set back the progression of the main one and impact stereodiscrimination. To exclude this scenario, 1.0 equiv of water was added to the reaction, but this had no further effect on the reaction.

With the optimized conditions in hand, we applied the reaction to different malonate derivatives by changing the R group of the ester moiety (entries 17−19). In these cases, the reactions were significantly slower compared to the hydrophosphination of **5a**; moreover, in the case of diisopropyl malonate **5c**, there was no product at all. In the case of **5b**, the yield was satisfactory (58%), but the selectivity was low (25%). Surprisingly, hydrophosphination of **5d** performed relatively well (64% yield and 61% ee), in spite of the presence of bulky benzyl groups on the substrate.

Although we concluded that the progress of the reaction stops after 3 days, as indicated by the presence of the unreacted starting materials in the reaction mixture, the addition of the metal source to form the metal P,N complex in situ to facilitate isolation was not favorable. Adding $Pd(MeCN)_2Cl_2$ and letting the mixture warm up to RT had to be avoided because the presence of metal and the higher temperature under basic conditions accelerated the reaction to total completion without selectivity. In light of this observation, we developed a workup process to facilitate the removal of residual reagents and additives before proceeding with metal complexation. The residual solvent as well as TEA was removed using a vacuum under inert conditions. Diphenylphosphine was subsequently removed by trituration with degassed hexane before filtration on a short Celite plug under nitrogen. The obtained P,N ligand **8** was subsequently added immediately to selected metal sources at low temperature (−80 °C) to allow complexation without further isolation.

With ligand **8** in hand, the complexation was carried out by adding the corresponding metal sources to a DCM solution of **8** at −80 °C and then the mixture was allowed to reach RT (Schemes 2 and 3). Chelation took place immediately in every case: the ligand could coordinate to the various metal sources employed, viz., $Pd(MeCN)_2Cl_2$, $Pt(MeCN)_2Cl_2$, $[Rh(COD)Cl]_2$, and $[Ir(COD)Cl]_2$ (COD = 1,5-cyclooctadiene), without any difficulty providing square-planar d^8 complexes.

Scheme 2. Complexation of Palladium 9 and Platinum 10 Metals with the P,N Ligand 8

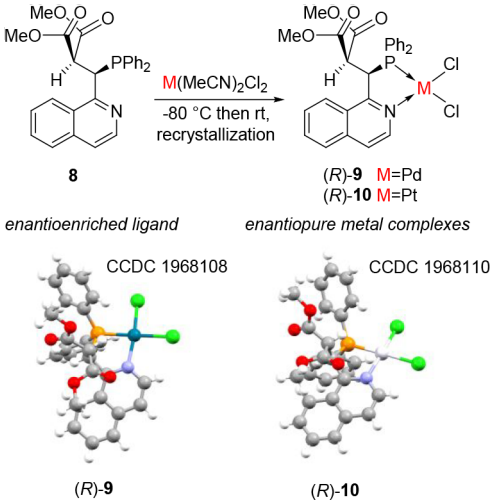

https://dx.doi.org/10.1021/acs.inorgchem.9b03549
Inorg. Chem. XXXX, XXX, XXX−XXX

Scheme 3. Reaction Scheme for Synthesizing Rh(COD) (13) and Ir(COD) (14) Complexes[a]

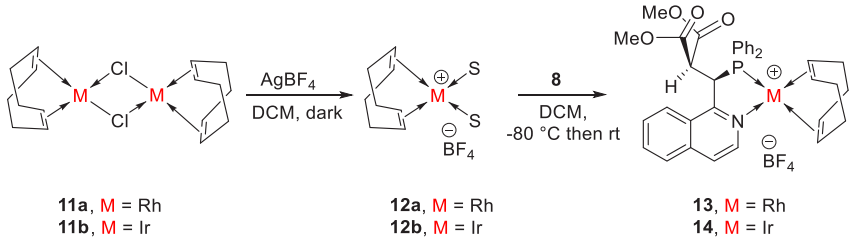

11a, M = Rh
11b, M = Ir

12a, M = Rh
12b, M = Ir

13, M = Rh
14, M = Ir

[a]S indicates solvent molecules.

Each coordination product exhibited characteristic signal(s) in $CDCl_3$ when $^{31}P\{^1H\}$ spectroscopy was used to monitor the progress of the complexation. For palladium complex **9**, a sharp singlet could be observed at 52.1 ppm ($CDCl_3$, 202 MHz). For complex **10**, the main resonance signal was at 28.7 ppm with two satellites: at 19.3 ppm and at 38.2 ppm ($^1J_{Pt-P}$= 3826.9 Hz, $CDCl_3$, 202 MHz) due to coupling between the NMR-active ^{195}Pt and ^{31}P nuclei.[25] Complexes **9** and **10** are stable in air and resistant to moisture; however, they decompose during column chromatography. In both cases, the crude complex could be purified by recrystallization in a DCM/diethyl ether system.

We also intended to synthesize P,N rhodium(I) and iridium(I) complexes with a COD ancillary ligand and a BF_4^- counterion in the outer coordinating sphere because this formula proved to be more stable than their chlorotriphenylphosphine counterparts (see Coordination Behavior of Complexes, complexes **20** and **21**). Before the addition to **8**, the chloro ligands of the $[M(COD)Cl]_2$ sources were removed by $AgBF_4$ (by stirring in degassed DCM in the dark for 2 h).[26] After filtration of intermediates **12a** and **12b** on short silica plugs, ligand **8** was added at low temperature (Scheme 3). It resulted in a singlet at 41.5 ppm in the case of the iridium complex (**14**) and a doublet at 49.7 ppm with a $^1J_{Rh-P}$ = 156.2 Hz ($CDCl_3$, 202 MHz) coupling constant in the case of the rhodium complex (**13**), which is in accordance with the literature[27]

Structural Determination and Conformational Analysis. As revealed by X-ray crystallography, the chiral complex **9** was successfully recrystallized from the enantioenriched mixture with a *R* absolute configuration [because the applied catalyst was (*S*)-**2**; Figure 4]. The measured Flack's parameter of the complex was 0.03(4).[28] The selected bond lengths, angles, and torsion angles are compiled in Table 2.

The four bonds that include palladium are significantly longer than the usual 1.5 Å C−C bond, which causes a slight elongation of the five-membered chelate ring. The bite angle of the P,N ligand is close to the preferred 90° in bidentate complexes;[1e,f,2d] however, it shows that the shape of the metal center differs from the ideal square-planar arrangement of the low-spin d^8 complexes. Another important observation is that the Pd−Cl bond length in the position trans to the nitrogen atom is significantly smaller than that in the analogous P,C chloro dimer complexes.[14a,21a]

When the chelate ring is observed from the aspect of bond angles, it can be seen that it has an envelope-like conformation (similarly to the cyclopentane C_s conformer), which is supported by the relatively large torsion angle (−24.17°) observed within C10−C9−N1−Pd1. This indicates that C10 is out of the mean coordination plane (m.c.pl., defined by P−Pd−N atoms). Because this carbon atom bears the dimethyl

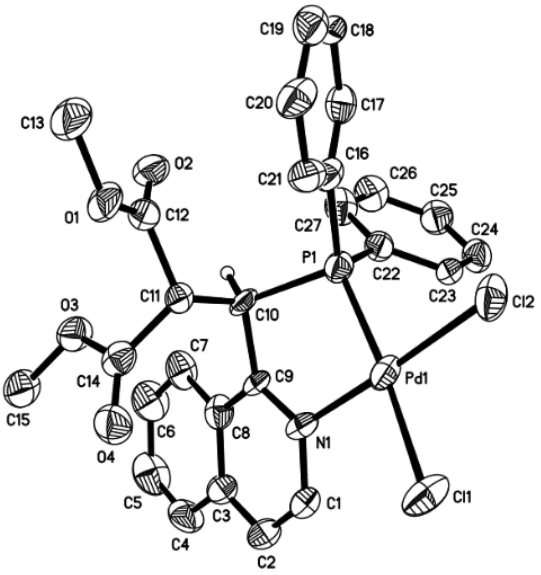

Figure 4. ORTEP image of complex (*R*)-**9**.

malonate moiety, the torsion values within C11−C10−P1−C22 (158.60°) and especially within Pd1−P1−C10−C11 (80.58°) support the fact that the bulky malonate group is positioned axially with respect to the m.c.pl. On the basis of these observations, we concluded that the P,N complex **9** with an *R* configuration prefers the *δ* conformation (Figure 5).

The structure of compound (*R*)-**9** was investigated further in solution by performing two-dimensional $^1H-^1H$ ROESY NMR spectroscopy. The two-dimensional spectrum of the complex can be seen in Figure 6.

According to the ROESY correlations, we can observe that five major interactions are occurring in the complex. Correlation A is not surprising at all because those protons are in vicinal coupling to each other. Cross-peak B between H_a and H_b is important; this means that, although the bulky malonate moiety in the axial position can rotate along the C−C bond, a steric block exists between that and the isoquinoline ring. Cross-peak F [interaction of H_d and the ortho protons of the axial phenyl group ($H_{ax\text{-}ortho}$)] can be explained by the conformational changes in solution. Nonetheless, the spatial proximity between H_a and the equatorial phenyl group's ortho protons ($H_{eq\text{-}ortho}$; C), H_b and the ortho protons of the axial phenyl group ($H_{ax\text{-}ortho}$; D), and H_c and the ortho protons equatorial phenyl group ($H_{eq\text{-}ortho}$; E) also confirm that the *δ* conformation is more likely in solution. Furthermore, the NOE signal E points at it unambiguously because if the *λ* conformation had any probability of occurring in solution, H_c would have had a correlation peak with the ortho protons

https://dx.doi.org/10.1021/acs.inorgchem.9b03549
Inorg. Chem. XXXX, XXX, XXX−XXX

Table 2. Selected Bond Lengths, Angles, and Torsion Angles Based on Crystallographic Analysis

bond	d/Å	bond	d/Å
Pd1−N1	2.054(8)	Pd1−P1	2.200(3)
Pd1−Cl1	2.370(3)	Pd1−Cl2	2.290(3)
C9−C10	1.510(13)	C9−N1	1.344(12)
C10−P1	1.849(10)		
bond	α/deg	bond	α/deg
N1−Pd1−P1	83.20(2)	N1−Pd1−Cl1	95.40(3)
P1−Pd1−Cl1	173.48(11)	N1−Pd1−Cl2	169.70(3)
P1−Pd1−Cl2	90.13(11)	Cl1−Pd1−Cl2	92.11(12)
C9−N1−Pd1−P1	−3.22	C10−C9−N1−Pd1	−24.17
C11−C10−P1−C22	−158.60	Pd1−P1−C10−C11	80.58

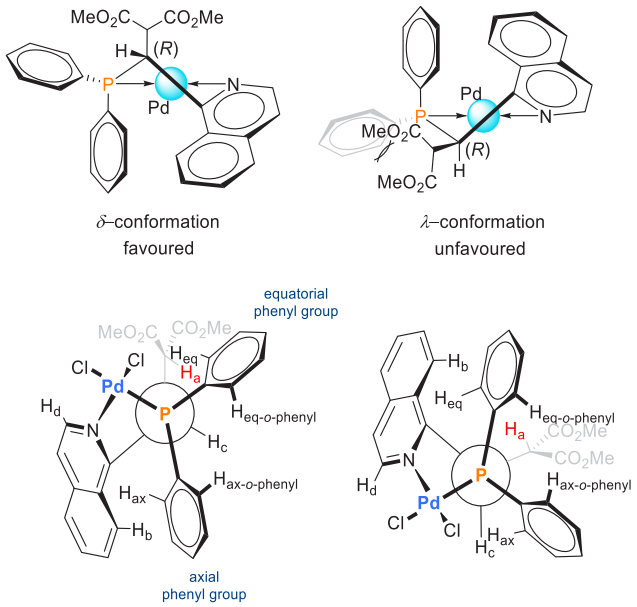

Figure 5. Preferred δ conformation of complex 9 shown by Sawhorse and Newman projections.

of the axial phenyl group, which is clearly absent in the spectrum.

Coordination Behavior of Complexes. Because the P,N bidentate ligand was developed based on the analogous P,C palladacycles, the change in the electronic effects of the coordinating moiety has to be taken into consideration. In order to scrutinize the difference in the trans influence between the coordinating aromatic nitrogen and carbon atoms, we compared the P,N system to its exact P,C analogue.[21a] The study was carried out by adding 1.0 equiv of the coordinating monodentate phosphine (PPh_3) to P,N and P,C complexes at RT, with stirring for 1 h in DCM. The reactions were monitored by $^{31}P\{^1H\}$ NMR spectroscopy (DCM, 162 MHz; Figures 7 and 8).

According to the determined coupling constants from $^{31}P\{^1H\}$ NMR spectroscopy, only cis coordination (the PPh_3 ligand prefers the cis position to the phosphorus atom of the chelate ligand) occurred when **9** and **10** complexes were the starting materials [$^2J_{P1-P2}$ = 7.3 Hz (**15**); $^2J_{P1-P2}$ = 13.3 Hz (**16**)].[25a]

Nevertheless, in the case of platinum, the obtained $^{31}P\{^1H\}$ NMR spectrum requires greater scrutiny: besides the starting material (**10**) and the coordination of triphenylphosphine (*cis*-**16**), significant dimerization occurred to give complex **17** as a major product. The coupling constants between the ^{31}P nucleus of the chelating ligand (P,N) and ^{195}Pt were generally high ($^1J_{Pt-P1}$ = 3693.6 Hz in the case of *cis*-**16** and $^1J_{Pt-P}$ = 3680.6 Hz for complex **17**), which indicates strong bonding between those atoms,[29] although the coupling constant value observed between the phosphorus nucleus of triphenylphosphine and the platinum center was slightly lower ($^1J_{Pt-P2}$ = 3445.6 Hz). It is worth mentioning that we observed that the concentrations of the dimer (**17**) and starting material (**10**) slowly increased in the mixture with respect to the coordination compound **16** (see the Supporting Information).

The P,C counterpart **18** (Figure 8), in contrast, showed a dynamic equilibrium between cis and trans P1−Pd−P2 coordination ($^2J_{P1-P2,trans}$ = 427.2 Hz and $^2J_{P1-P2,\ cis}$ = 26.5 Hz), although trans proved to be the favored arrangement (**19**).

This can be explained by the difference between the trans influences of the coordinating nitrogen and sp^2 carbon atoms. Phosphorus and carbon atoms are both at the end of the trans influence series and have a strong labilizing effect[30] compared to the nitrogen atom. In a P,N complex, a trans P−M−P arrangement is less favorable than P−M−N; hence, despite the significant steric repulsion, we could observe the cis isomer being formed. Regarding P,C coordination, carbon has an even stronger labilizing effect at the trans position than phosphorus; thus, P−M−P arrangement (trans) is still benign. Moreover, it is also preferred from the point of view of steric effects.

To support this explanation, we investigated the difference in π acidity between the coordinating carbon and nitrogen (as part of the aromatic moieties) with the use of DFT calculations performed by applying *Gaussian 09*.[31] For this purpose, we carried out NBO[32] analysis on complexes **9**, **10**, and **18** and examined the highest occupied molecular orbital (HOMO)−lowest unoccupied molecular orbital (LUMO) interaction energies between the metals' corresponding d orbitals (HOMO) and the aromatic C═N and C═C aromatic π*-antibonding (LUMO) orbitals (Figure 9).

DFT calculations were performed by using the B3LYP functional.[33] On palladium and platinum atoms, the SDD effective core potential was used. On other atoms, the 6-31G* basis set was applied.[34] The calculated interaction energies can be seen in Table 3.

According to the analysis, the aforementioned interactions are more significant in the case of palladacycle **18** than in that of the P,N palladium complex **9**, which means that the π acidity of the coordinating carbo-aromatic naphthyl moiety is more significant. This, in turn, explains the stronger trans influence of the coordinating aromatic carbon observed in the coordination study. In the case of platinum (complex **10**), this

https://dx.doi.org/10.1021/acs.inorgchem.9b03549
Inorg. Chem. XXXX, XXX, XXX−XXX

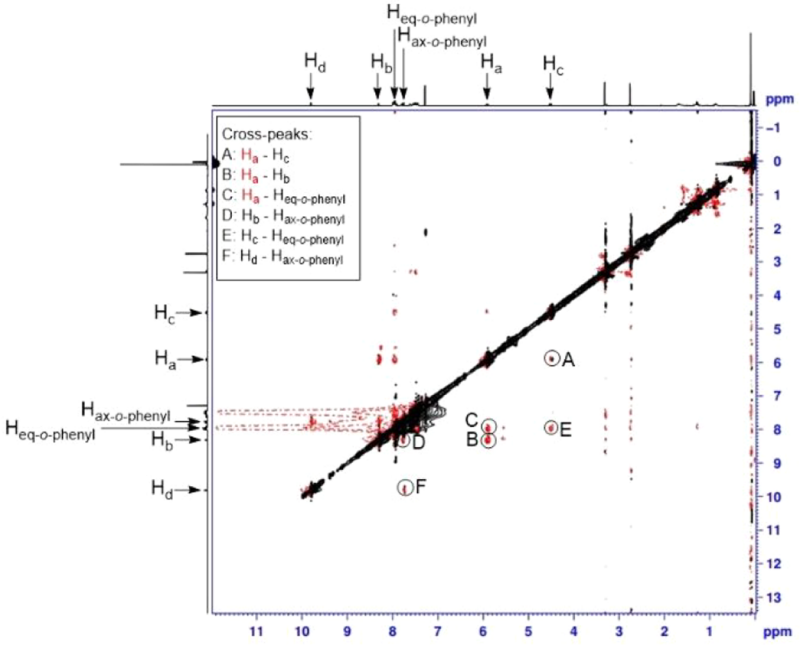

Figure 6. $^{1}H-^{1}H$ ROESY NMR spectrum of the palladium complex (*R*)-**9**. Selected NOE interactions: A, H_a-H_c; B, H_a-H_b; C, H_a-H (equatorial phenyl ortho protons); D, H_b-H (axial phenyl ortho protons); E: H_c-H (equatorial phenyl ortho protons); F: H_d-H (axial phenyl ortho protons).

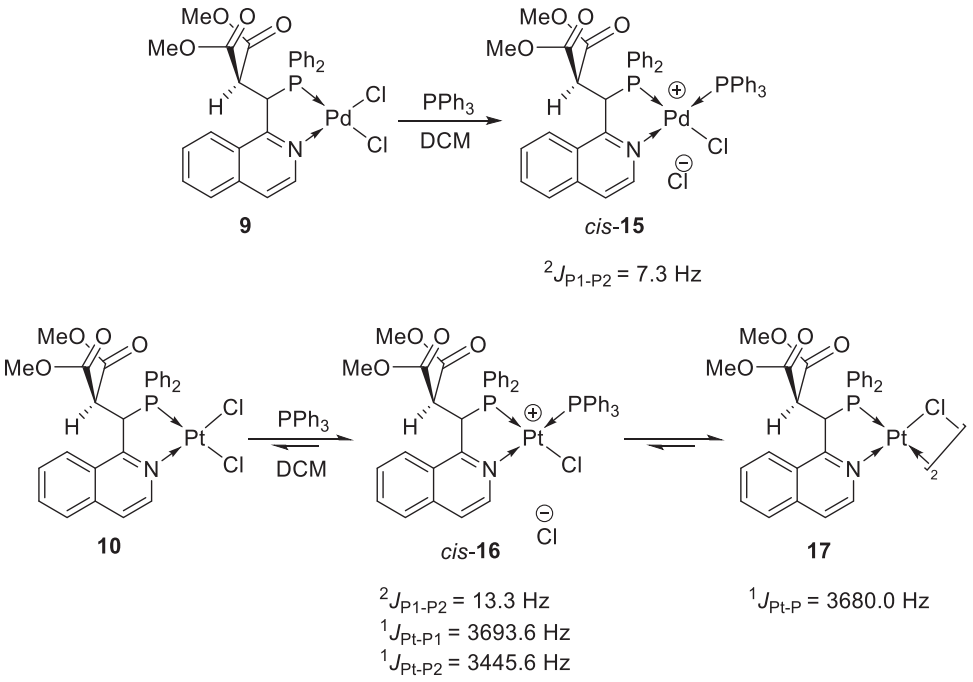

Figure 7. Investigations on the coordination behavior of **9** and **10** by adding triphenylphosphine to their solution. P1 is the P,N ligand's phosphorus atom, and P2 is the triphenylphosphine's phosphorus atom.

energy is relatively high compared to its P,N palladium analogue (**9**), but it can be explained by the difference between the palladium and platinum atoms: platinum's 5d atomic orbitals are at higher energy levels and are more diffuse than palladium's 4d orbitals. Thus, they are able to donate more efficiently to the heteroaromatic ligand's antibonding orbitals.

To further investigate the electronic effects of the P,N ligand in regard to other transition metals, we performed the same experiment with rhodium and iridium complexes by adding 0.5 equiv of $[Rh(ethylene)Cl]_2$ and $[Ir(COD)Cl]_2$ to ligand **8** to form the respective P,N complexes. We subsequently added 1.0 equiv of triphenylphosphine to the mixtures at RT, and they were stirred for 1.0 h to observe the coordination behavior (complexes **20** and **21** in Figure 10).

In the case of rhodium (**20**), the coupling between the three NMR-active nuclei (^{103}Rh and the two ^{31}P nuclei) caused a characteristic pattern (doublet of doublets) in the NMR spectrum. The $^{31}P-^{31}P$ coupling constants were $^{2}J_{P1-P2}$ = 41.6

https://dx.doi.org/10.1021/acs.inorgchem.9b03549
Inorg. Chem. XXXX, XXX, XXX−XXX

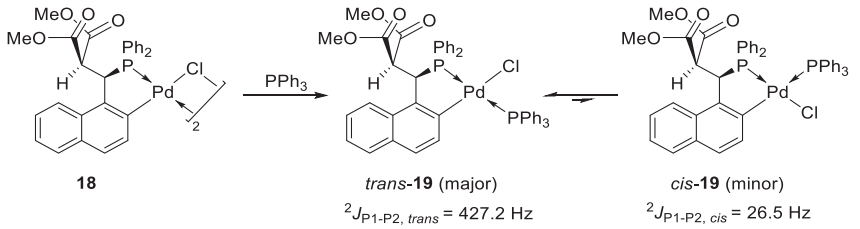

Figure 8. P,C palladium complex **18** (analogue of the P,N palladium complex) after the addition of triphenylphosphine.

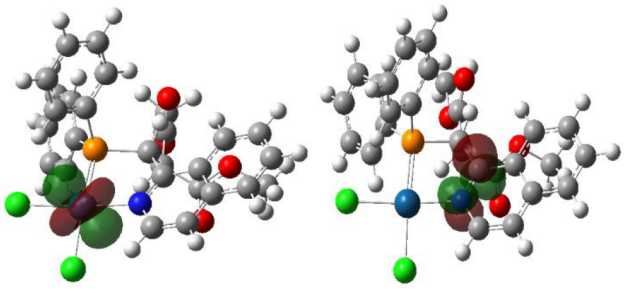

Figure 9. Selected interacting d(Pt)−π*(C═N) orbitals in complex **10**.

Table 3. Sum of the d(Metal)−π*(Aromatic) Interaction Energies in P,N and P,C Complexes

metal complex	$E_{d-\pi^*\ interaction}$/kcal/mol
9	1.94
10	4.45
18	4.72

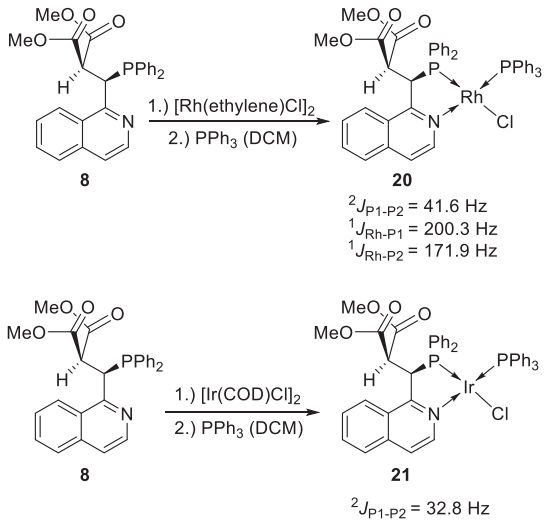

Figure 10. Rhodium and iridium P,N complexes after the addition of triphenylphosphine. P1 is the P,N ligand's phosphorus atom, and P2 is the triphenylphosphine's phosphorus atom.

Hz (75.2 ppm, doublet of doublets; 46.2 ppm, doublet of doublets; 162 MHz, DCM), which are typical values when cis coordination occurs.[35] The ^{103}Rh−^{31}P couplings are also consistent with the literature values: $^{1}J_{Rh-P1}$ = 200.3 Hz and $^{1}J_{Rh-P2}$ = 171.9 Hz, where P1 refers to the P,N ligand's phosphorus atom and P2 refers to the triphenylphosphine's phosphorus atom.[27,35]

Complex **21** also showed cis coupling with $^{2}J_{P1-P2}$= 32.8 Hz (32.1 ppm, doublet; −30.3 ppm, doublet; 162 MHz, DCM)[36] with respect to the coordinating phosphorus atoms, which is not surprising if we consider the electronic effects discussed earlier. Nevertheless, as revealed by ^{31}P{^{1}H} NMR spectroscopy, the lability and air sensitivity of complexes **20** and **21** are higher than we could experience in the case of complexes **13** and **14**.

As aforementioned in the Synthetic Scheme section, conversion of the asymmetric hydrophosphination reached its maximum and did not increase beyond a certain point. To explain this observation, we hypothesized that the P,N bidentate **8** formed can coordinate to the (*S*)-**2** catalyst and obstruct the progress of catalysis. In order to support our hypothesis, we decided to add (*R*)-**1** C,N palladacycle complex in situ to the reaction mixture of the hydrophosphination of **5a** once the maximum conversion was attained (the conditions were the same as those at entry 8 in Table 1; Figure 11).

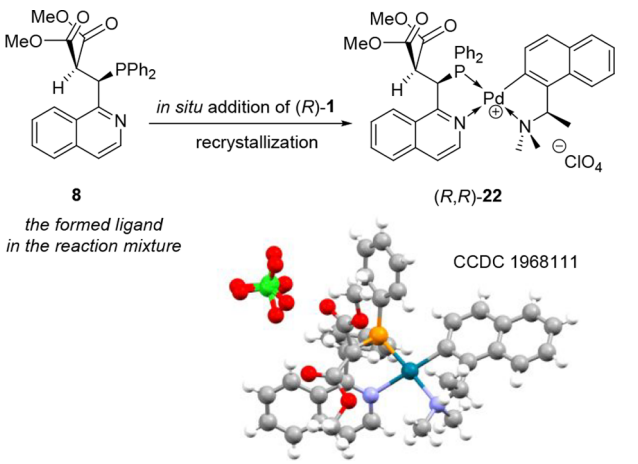

Figure 11. In situ addition of the (*R*)-**1** chiral auxiliary to the forming P,N ligand.

The resulting complex **22** could be isolated, and it was recrystallized to obtain the pure *R,R* diastereomer (Figure 11). The formation of this structure proved our hypothesis that the bidentate P,N ligand was indeed able to undergo chelation with catalysts possessing at least two free coordination sites.

From the coordination point of view, this structure also proves our observations on the steric and electronic effects as well; i.e., it is favorable that the two nitrogen atoms are in pairwise trans position to the carbon and phosphorus atoms to avoid the less favored P−Pd−C(sp^2) arrangement.

CONCLUSION

A new class of chiral and enantioenriched P,N transition-metal complexes was synthesized and investigated from conformational, coordination, and electronic points of view. The synthesis of the P,N heterobidentate ligand was carried out

https://dx.doi.org/10.1021/acs.inorgchem.9b03549
Inorg. Chem. XXXX, XXX, XXX−XXX

catalytically by employing the phosphapalladacycle-catalyzed asymmetric hydrophosphination protocol. By overcoming the challenges posed by potential catalyst poisoning due to the product chelation in the catalytic step, we obtained palladium, platinum, rhodium, and iridium complexes, which can be starting points for new catalyst designs in the future. With rhodium and iridium complexes, we have also demonstrated that this ligand system can be applicable for the synthesis of metal complexes with less stable oxidation states. Conformational analysis revealed that the coordinated P,N ligand has a well-defined spatial arrangement, while the coordination study carried out on various metals showed that its electronic effects differ from their P,C bidentate counterparts.

The information gained and collected in this study can play an important role in the design of new heterobidentate chiral P,N-type transition-metal catalysts. Investigation of the catalytic activity of the synthesized complexes is still in progress.

EXPERIMENTAL SECTION

General Considerations. For the preparation and handling of air-sensitive phosphines and complexes, positive nitrogen and argon flows were used (standard Schlenk techniques). Solvents were degassed previously for all reactions and measurements when necessary. Reagents for carrying out synthetic steps were purchased from Sigma-Aldrich, TCI, Strem, Alfa Aesar, and Acros Organics. Purifications by flash column chromatography was carried out on a Merck Silica Gel 60. For the NMR data, Bruker AV500 (^{1}H, 500.1 MHz; ^{13}C, 125.7 MHz; ^{19}F, 470.6 MHz; ^{31}P, 202.4 MHz), Bruker AV400 and BBFO 400 (^{1}H. 400.1 MHz; ^{13}C, 100.6 MHz; ^{19}F, 376.5 MHz; ^{31}P, 162.0 MHz) instruments were used for the characterization of new compounds and a study of the coordination. Chemical shifts were reported in parts per million by using the internal standard tetramethylsilane for ^{1}H NMR measurements, $CDCl_3$ for ^{13}C NMR measurements, external standard H_3PO_4 for ^{31}P NMR measurements, and $CFCl_3$ for ^{19}F NMR measurements. High-resolution mass spectrometry (HRMS) data were recorded on a Waters Q-TOF Premier spectrometer by using electrospray ionization (ESI) positive mode. Elemental analysis was carried out on a PerkinElmer CHNS/O series II 2400 EA instrument. The determination of ee was performed on an Agilent 1200 series chromatograph with Daicel Chiralpack ID and IF columns in an *n*-hexane−isopropyl alcohol solvent system. Optical rotation measurements were performed on a Jasco P-1030 polarimeter using the D lines of sodium (589 nm) as the light source. ***Caution!*** *Perchlorate salts of metal complexes are dangerous because they are potentially explosive. These chemicals must be handled with care.*

Preparation of Dimethyl 2-(Isoquinolin-1-ylmethylene)-malonate (5a). Carbadehyde **4** (5.60 mmol, 0.89 g, 1.0 equiv) and dimethyl malonate (6.52 mmol, 0.86 g, 1.15 equiv) were dissolved in 40.0 mL of benzene and heated to reflux temperature. *N*-Methylpiperidine (0.85 mmol, 0.08 g, 0.15 equiv) and benzoic acid (0.42 mmol, 0.05 g, 0.075 equiv) were dissolved in 10.0 mL of benzene and added to the boiling solution of the starting material and malonate. The solution was refluxed overnight with the use of a Dean−Stark apparatus and 4 Å molecular sieve. After the reaction was complete, saturated aqueous sodium bicarbonate was added to the solution and extracted with DCM. The combined organic layer was washed with brine, dried, and evaporated. The residue was purified with column chromatography on silica gel (4:1 to 2:1 *n*-hexane/ethyl acetate) to afford the pure diester.

Yield: 52%, yellow-brown solid. ^{1}H NMR (500 MHz, $CDCl_3$): δ 8.57 (s, 1H, Ar*H*), 8.55 (d, $^{3}J_{H-H}$ = 5.5 Hz, 1H, Ar*H*), 8.31 (d, $^{3}J_{H-H}$ = 8.4 Hz, 1H, Ar*H*), 7.87 (d, $^{3}J_{H-H}$ = 8.0 Hz, 1H, C=C*H*Ar), 7.78−7.60 (m, 3H, Ar*H*), 3.92 (s, 3H, COOCH_3), 3.90 (s, 3H, COOCH_3). ^{13}C NMR (126 MHz, $CDCl_3$): δ 167.22 (s, 1C, *C*=O), 164.43 (s, 1C, *C*=O), 150.11 (s, 1C, N=*C*CH), 142.40 (s), 136.54 (s), 136.11 (s), 130.39 (s), 130.30 (s), 128.23 (s), 127.78 (s), 127.53 (s), 123.89 (s), 122.49 (s), 52.92 (s, 1C, COO*C*H$_3$), 52.45 (s, 1C, COO*C*H$_3$). HRMS (+ESI). Calcd for $C_{15}H_{14}NO_4$ [(M + H)$^+$]: *m*/*z* 272.0923. Found: *m*/*z* 272.0923. Anal. Calcd for $C_{15}H_{13}NO_4$: C, 66.41; H, 4.83; N, 5.16. Found: C, 66.15; H, 4.15; N, 5.16.

General Procedure for the Preparation of Diethyl, Diisopropyl, and Dibenzyl 2-(Isoquinolin-1-ylmethylene)-malonates (5b−5d). $TiCl_4$ (2.0 mmol, 2.1 equiv) was dissolved in 1.5 mL of CCl_4, and this solution was added dropwise to 12 mL of tetrahydrofuran (THF) at 0 °C. When the yellow adduct appeared, carbaldehyde **4** (0.95 mmol, 1.0 equiv) and the corresponding malonate (0.95 mmol, 1.0 equiv) were dissolved in 2.0 mL of THF and added to the $TiCl_4$ solution dropwise. A THF solution of pyridine (16.0 mmol, 16.6 equiv) was also added to the reaction mixture, which then was stirred under nitrogen at 0 °C for 1 h and further at RT until the reaction was complete. Upon completion, the reaction mixture was quenched with 10.0 mL of H_2O, and then 20.0 mL of ethyl acetate and Na_2CO_3(aq) were added (to adjust the pH to neutral), and the solution was extracted with ethyl acetate. The organic layer was further washed with $NaHCO_3$ and brine, then dried, and evaporated. The resulting diester was the purified by column chromatography on silica gel (5:1 to 1:1 *n*-hexane/ethyl acetate) to obtain the pure product.

*Diethyl 2-(Isoquinolin-1-ylmethylene)malonate (**5b**).* Yield: 29%, brown oil. ^{1}H NMR (500 MHz, $CDCl_3$): δ 8.53 (d, $^{3}J_{H-H}$ = 5.6 Hz, 1H, Ar*H*), 8.52 (s, 1H, Ar*H*), 8.28 (d, $^{3}J_{H-H}$ = 8.5 Hz, 1H, Ar*H*), 7.85 (d, $^{3}J_{H-H}$ = 8.0 Hz, 1H, C=C*H*Ar), 7.74−7.62 (m, 3H, Ar*H*), 4.39 (q, $^{3}J_{H-H}$ = 7.2 Hz, 2H, OCH_2CH$_3$), 4.37 (q, $^{3}J_{H-H}$ = 7.2 Hz, 2H, OCH_2CH$_3$), 4.22 (q, $^{3}J_{H-H}$ = 7.15 Hz, 1H), 1.38 (t, $^{3}J_{H-H}$ = 7.2 Hz, 3H, OCH$_2$CH_3), 1.31 (t, $^{3}J_{H-H}$ = 7.15 Hz, 3H, OCH$_2$CH_3), 1.24 (t, $^{3}J_{H-H}$ = 7.1 Hz, 1H). ^{13}C NMR (126 MHz, $CDCl_3$): δ 166.57 (1C, *C*=O), 164.05 (1C, *C*=O), 150.44 (1C, N=CCH), 142.21 (s), 136.47 (s), 135.52 (s), 131.17 (s), 130.32 (s), 128.12 (s), 127.68 (s), 127.48 (s), 123.99 (s), 122.29 (s), 61.90 (1C, COO*C*H$_2$CH$_3$), 61.34 (1C, COO*C*H$_2$CH$_3$), 14.16 (1C, COOCH$_2$*C*H$_3$), 14.03 (1C, COOCH$_2$*C*H$_3$). HRMS (+ESI). Calcd for $C_{17}H_{18}NO_4$ [(M + H)$^+$]: *m*/*z* 300.1236. Found: *m*/*z* 300.1236.

*Diisopropyl 2-(Isoquinolin-1-ylmethylene)malonate (**5c**).* Yield: 38%, brown oil. ^{1}H NMR (400 MHz, $CDCl_3$): δ 8.52 (d, $^{3}J_{H-H}$ = 5.6 Hz, 1H, Ar*H*), 8.47 (s, 1H, Ar*H*), 8.29 (d, $^{3}J_{H-H}$ = 8.5 Hz, 1H, Ar*H*), 7.85 (d, $^{3}J_{H-H}$ = 7.6 Hz, 1H, Ar*H*), 7.76−7.63 (m, 3H, Ar*H*), 5.32 (hept, $^{3}J_{H-H}$ = 6.3 Hz, 1H, COOC*H*(CH$_3$)$_2$), 5.22 (hept, $^{3}J_{H-H}$ = 6.2 Hz, 1H, COOC*H*(CH$_3$)$_2$), 1.36 (d, $^{3}J_{H-H}$ = 6.3 Hz, 6H, COOCH-(CH_3)$_2$), 1.32 (d, $^{3}J_{H-H}$ = 6.2 Hz, 6H, COOCH(CH_3)$_2$), 1.28−1.20 (m, 1H), 1.16 (d, $^{3}J_{H-H}$ = 6.3 Hz). ^{13}C NMR (126 MHz, $CDCl_3$): δ 166.00 (s, 1C, *C*=O), 163.60 (s, 1C, *C*=O), 150.66 (s, 1C, N=*C*CH), 142.05 (s), 136.44 (s), 134.92 (s), 131.97 (s), 130.27 (s), 128.04 (s), 127.63 (s), 127.45 (s), 124.09 (s), 122.16 (s), 69.59 (s), 69.54 (s, 1C, COO*C*H(CH$_3$)$_2$), 68.77 (s), 68.69 (s, 1C, COO*C*H-(CH$_3$)$_2$), 21.78 (s, 2C, COOCH(*C*H$_3$)$_2$), 21.61 (s, 2C, COOCH-(*C*H$_3$)$_2$). HRMS (+ESI). Calcd for $C_{19}H_{22}NO_4$ [(M + H)$^+$]: *m*/*z* 328.1549. Found: *m*/*z* 328.1548.

*Dibenzyl 2-(Isoquinolin-1-ylmethylene)malonate (**5d**).* Yield: 22%, brown solid. ^{1}H NMR (500 MHz, $CDCl_3$): δ 8.57 (s, 1H, Ar*H*), 8.33 (d, $^{3}J_{H-H}$ = 5.5 Hz, 1H, Ar*H*), 8.26 (d, $^{3}J_{H-H}$ = 8.4 Hz, 1H, Ar*H*), 7.84 (d, $^{3}J_{H-H}$ = 8.1 Hz, 1H, C=C*H*Ar), 7.74−7.58 (m, 3H, Ar*H*), 7.42−7.33 (m, 5H, Ar*H*), 7.33−7.26 (m, 6H, Ar*H*), 5.35 (s, 2H, benzyl CH_2), 5.34 (s, 2H, benzyl CH_2). ^{13}C NMR (126 MHz, $CDCl_3$): δ 166.44 (s, 1C, *C*=O), 163.82 (s, 1C, *C*=O), 150.07 (s, 1C, N=*C*CH), 142.29 (s), 136.48 (s), 136.35 (s), 135.59 (s), 135.49 (s), 130.43 (s), 130.35 (s), 128.66 (s), 128.63 (s), 128.50 (s), 128.44 (s), 128.31 (s), 128.20 (s), 128.17 (s), 128.14 (s), 128.05 (s), 128.00 (s), 127.71 (s), 127.51 (s), 127.25 (s), 123.90 (s), 122.42 (s), 67.38 (s, 1C, benzyl *C*H$_2$), 67.22 (s, 1C, benzyl *C*H$_2$). HRMS (+ESI). Calcd for $C_{27}H_{22}NO_4$ [(M + H)$^+$]: *m*/*z* 424.1549. Found: *m*/*z* 424.1549.

General Procedure for Catalytic Hydrophosphination on Dialkyl and Diaralkyl 2-(Diphenylphosphorothioyl)-(isoquinolin-1-ylmethylene)malonates (Optimization of Conditions; 6a−6c). Diphenylphosphine (0.05 mmol, 9.31 mg, 1.0 equiv) was weighed into a Schlenk flask under positive nitrogen flow, and 2.0 mL of the previously degassed solvent was added. The

https://dx.doi.org/10.1021/acs.inorgchem.9b03549
Inorg. Chem. XXXX, XXX, XXX−XXX

malonate substrate (0.05 mmol, 1.0 equiv) and catalyst (0.0025 mmol, 0.05 equiv) were added to the solution, and then the required temperature was adjusted. When the required temperature was reached, a base (0.05 mmol, 1.0 equiv) was added dropwise to the reaction mixture. The reaction was monitored by $^{31}P\{^{1}H\}$ NMR spectroscopy. Upon completion of the reaction, excess sulfur was added, the mixture was allowed to warm up, and the volatiles were evaporated. The residue was purified by column chromatography on silica gel (5:1 to 2:1 *n*-hexane/ethyl acetate) to obtain the pure sulfurized phosphine product.

*Dimethyl 2-(Diphenylphosphorothioyl)(isoquinolin-1-ylmethyl)-malonate (**6a**).* Yield: 86%, pale-yellow solid. ^{1}H NMR (500 MHz, $CDCl_3$): δ 8.40 (d, $^{3}J_{H-H}$ = 5.6 Hz, 1H, Ar*H*), 8.11 (dd, $^{3}J_{H-H}$ = 11.6 and 7.0 Hz, 2H, Ar*H*), 8.02 (d, $^{3}J_{H-H}$ = 8.3 Hz, 1H, Ar*H*), 7.57 (d, $^{3}J_{H-H}$ = 8.1 Hz, 1H, Ar*H*), 7.51−7.37 (m, 7H, Ar*H*), 7.35 (d, $^{3}J_{H-H}$ = 5.0 Hz, 1H, Ar*H*), 7.04 (t, $^{3}J_{H-H}$ = 6.7 Hz, 1H, Ar*H*), 6.91 (m, 2H, Ar*H*), 5.83 (t, $^{3}J_{H-H}$, $^{3}J_{H-P}$ = 10.2 Hz, 1H, C*H*CH(PPh$_2$)Ar), 5.28 (t, $^{3}J_{H-H}$, $^{2}J_{H-P}$ = 10.7 Hz, 1H, CHC*H*(PPh$_2$)Ar), 3.37 (s, 3H, COOCH_3), 3.36 (s, 3H, COOCH_3). ^{13}C NMR (126 MHz, $CDCl_3$): δ 168.46−168.11 (m, 2C, C═O), 155.43 (d, $^{2}J_{P-C}$ = 6.6 Hz, 1C, Ar, N═CC(H)P), 141.29 (d, J_{P-C} = 3.0 Hz, 1C), 135.90, 132.46 (d, $^{1}J_{P-C}$ = 9.7 Hz, 1C, Ar, PC_6H_5), 131.93 (d, $^{1}J_{P-C}$ = 10.1 Hz, 1C, Ar, PC_6H_5), 131.61 (s), 131.10 (s), 130.96 (s), 130.86 (s), 130.48 (s), 130.31 (s), 129.53 (s), 128.21 (d, J_{P-C} = 12.0 Hz), 128.00 (s), 127.40 (s), 127.31 (s), 127.17 (s), 127.14 (s), 124.50 (s), 120.13 (s), 54.40 (d, $^{2}J_{P-C}$ = 3.0 Hz, 1C, *C*HCH(PPh$_2$)Ar), 52.63 (s, 2C, COO*C*H$_3$), 44.84 (d, $^{1}J_{P-C}$ = 47.3 Hz, 1C, *C*HCH(PPh$_2$)Ar). $^{31}P\{^{1}H\}$ NMR (202 MHz, $CDCl_3$) δ 48.73 (s). HRMS (+ESI). Calcd for $C_{27}H_{25}NO_4PS$ [(M + H)$^+$]: *m*/*z* 490.1242. Found: *m*/*z* 490.1240. Anal. Calcd for $C_{27}H_{24}NO_4PS$: C, 66.25; H, 4.94; N, 2.86. Found: 65.73; H, 4.80; N, 2.99.

*Diethyl 2-(Diphenylphosphorothioyl)(isoquinolin-1-ylmethyl)-malonate (**6b**).* Yield: 58%, yellow solid. ^{1}H NMR (500 MHz, $CDCl_3$): δ 8.39 (d, $^{3}J_{H-H}$ = 5.6 Hz, 1H, Ar*H*), 8.10 (dd, $^{3}J_{H-H}$ = 12.1 Hz, $^{3}J_{H-H}$ = 7.3 Hz, 2H, Ar*H*), 8.05 (d, $^{3}J_{H-H}$ = 8.4 Hz, 1H, Ar*H*), 7.57 (d, $^{3}J_{H-H}$ = 8.0 Hz, 1H, Ar*H*), 7.53−7.36 (m, 7H, Ar*H*), 7.34 (d, $^{3}J_{H-H}$ = 5.2 Hz, 1H, Ar*H*), 7.05 (t, $^{3}J_{H-H}$ = 7.0 Hz, 1H, Ar*H*), 6.94 (d, $^{3}J_{H-H}$ = 5.2 Hz, 2H, Ar*H*), 5.85 (t, $^{3}J_{H-H}$, $^{3}J_{H-P}$ = 10.3 Hz, 1H C*H*CH(PPh$_2$)Ar), 5.22 (t, $^{3}J_{H-H}$, $^{2}J_{H-P}$ = 10.8 Hz, 1H, CHC*H*(PPh$_2$)Ar), 3.95−3.63 (m, 4H, COOCH_2CH$_3$), 1.10 (t, $^{3}J_{H-H}$ = 7.1 Hz, 3H, COOCH$_2$CH_3), 0.76 (t, $^{3}J_{H-H}$ = 7.0 Hz, 3H, COOCH$_2$CH_3). ^{13}C NMR (126 MHz, $CDCl_3$): δ 167.79−167.08 (m, 2C, C═O), 155.79 (d, $^{2}J_{P-C}$ = 6.0 Hz, 1C, Ar, N═CC(H)P), 141.31 (d, J_{P-C} = 2.9 Hz), 135.86 (s), 132.45 (d, $^{1}J_{P-C}$ = 9.7 Hz, 1C, Ar, PC_6H_5), 132.03 (d, $^{1}J_{P-C}$ = 10.0 Hz, 1C, Ar, PC_6H_5), 131.50 (s), 130.78 (s), 129.49 (s), 128.11 (d, J_{P-C} = 12.1 Hz), 127.34 (d, J_{P-C} = 12.2 Hz), 124.63 (s), 119.96 (s), 61.82 (s, 1C, COOCH$_2$CH$_3$), 61.41 (s, 1C, COOCH$_2$CH$_3$), 54.93 (d, $^{2}J_{P-C}$ = 2.8 Hz, 1C, *C*HCH(PPh$_2$)-Ar), 44.80 (d, $^{1}J_{P-C}$ = 47.3 Hz, 1C, *C*HCH(PPh$_2$)Ar), 13.71 (s, 1C, COOCH$_2$CH$_3$), 13.65 (s, 1C, COOCH$_2$CH$_3$). $^{31}P\{^{1}H\}$ NMR (202 MHz, $CDCl_3$): δ 48.81 (s). HRMS (+ESI). Calcd for $C_{29}H_{29}NO_4PS$ [(M + H)$^+$]: *m*/*z* 518.1555. Found: *m*/*z* 518.1555.

*Dibenzyl 2-(Diphenylphosphorothioyl)(isoquinolin-1-ylmethyl)-malonate (**6c**).* Yield: 64%, yellow solid. ^{1}H NMR (500 MHz, $CDCl_3$): δ 8.31 (d, $^{3}J_{H-H}$ = 5.6 Hz, 1H, Ar*H*), 8.05 (dd, $^{3}J_{H-H}$ = 12.2 Hz, $^{3}J_{H-H}$ = 7.6 Hz, 2H, Ar*H*), 7.97 (d, $^{3}J_{H-H}$ = 8.3 Hz, 1H, Ar*H*), 7.58−7.27 (m, 14H, Ar*H*), 7.25−7.19 (m, 2H, Ar*H*), 7.15 (t, $^{3}J_{H-H}$ = 7.4 Hz, 1H, Ar*H*), 7.07 (t, $^{3}J_{H-H}$ = 7.5 Hz, 2H, Ar*H*), 7.05 (s, 1H, Ar*H*), 6.92 (m, 2H, Ar*H*), 6.83 (d, $^{3}J_{H-H}$ = 7.3 Hz, 2H, Ar*H*), 5.87 (t, $^{3}J_{H-H}$, $^{3}J_{H-P}$ = 10.4 Hz, 1H, C*H*CH(PPh$_2$)Ar), 5.39 (t, $^{3}J_{H-H}$, $^{2}J_{H-P}$ = 10.7 Hz, 1H, CHC*H*(PPh$_2$)Ar), 4.85−4.77 (m, 2H, benzyl CH_2), 4.72 (s, 2H, benzyl CH_2). ^{13}C NMR (126 MHz, $CDCl_3$): δ 167.79−167.08 (m, 2C, C═O), 155.46 (d, $^{2}J_{P-C}$ = 6.2 Hz, 1C, Ar, N═*C*C(H)P), 141.27 (d, J_{P-C} = 3.0 Hz), 135.87 (s), 135.29 (s), 134.86 (s), 132.42 (d, $^{1}J_{P-C}$ = 9.4 Hz 1C, Ar, PC_6H_5), 132.08 (d, $^{1}J_{P-C}$ = 9.9 Hz, 1C, Ar, PC_6H_5), 131.48 (d, J_{P-C} = 2.8 Hz), 130.80 (s), 130.32 (s), 129.46 (s), 128.35 (s), 128.19 (s), 128.07 (s), 127.99 (s), 127.94 (s), 127.90 (s), 127.87 (s), 127.36 (d, J_{P-C} = 12.4 Hz), 127.09 (s), 124.58 (s), 120.03 (s), 67.30 (s, 1C, benzyl *C*H$_2$), 67.12 (s, 1C, benzyl *C*H$_2$), 54.89 (d, $^{2}J_{P-C}$ = 3.0 Hz, 1C, *C*HCH(PPh$_2$)Ar), 45.15 (d, $^{1}J_{P-C}$ = 45.7 Hz, 1C, CHCH(PPh$_2$)Ar). $^{31}P\{^{1}H\}$ NMR (202 MHz, $CDCl_3$): δ 48.66 (s). HRMS (+ESI). Calcd for $C_{39}H_{33}NO_4PS$ [(M + H)$^+$]: *m*/*z* 642.1868. Found: *m*/*z* 642.1865.

General Procedure for Generating P,N Dichloropalladium and -Platinum Complexes [(*R*)-9 and (*R*)-10]. Diphenylphosphine (0.17 mmol, 0.032 g, 1.0 equiv) was weighed into a Schlenk flask under positive nitrogen flow, and 7.0 mL of the previously degassed DCM was added. Substrate **5a** (0.17 mmol, 0.046 g, 1.0 equiv) and (*S*)-**2** catalyst (0.0085 mmol, 0.005 g, 0.05 equiv) were added to the solution, and then the mixture was cooled to −80 °C. When the required temperature was reached, TEA (0.17 mmol, 0.017 g, 1.0 equiv) was added dropwise to the reaction mixture. After the reaction reached the desired conversion, TEA and the solvent were removed by using a nitrogen flow and vacuum, while the low temperature was permanently maintained. The residue was then triturated four times with degassed hexane to remove excess diphenylphosphine. The crude material was redissolved in DCM and filtered through a short Celite plug under Schlenk conditions. $MCl_2(MeCN)_2$ (0.17 mmol, 1.0 equiv) was then added to the free P,N ligand **8** at −80 °C, stirred for 1 h, and allowed to reach RT. Each of the resulting air-stable complexes was filtered through a short Celite plug and recrystallized from DCM with diethyl ether to afford enantiopure crystals.

*(R)-κ^2-P,N-[Dimethyl 2-(diphenylphosphanyl)(isoquinolin-1-ylmethyl)malonate]dichloropalladium(II) [(R)-**9**].* Yield: 85%, yellow solid. $[\alpha]^{25}_{D}$ = −479 (*c* 1.0, CH_2Cl_2). ^{1}H NMR (500 MHz, $CDCl_3$): δ 9.79 (d, $^{3}J_{H-H}$ = 6.6 Hz, 1H, Ar*H*, HC═C*H*N), 8.29 (d, $^{3}J_{H-H}$ = 8.6 Hz, 1H, Ar*H*), 8.02−7.86 (m, 7H, Ar*H*), 7.81−7.70 (m, 2H, Ar*H*), 7.59 (t, $^{3}J_{H-H}$ = 6.9 Hz, 2H, Ar*H*), 7.53 (t, $^{3}J_{H-H}$ = 7.6 Hz, 2H, Ar*H*), 7.48 (td, $^{3}J_{H-P}$ = 7.7 Hz, $^{3}J_{H-H}$ = 2.7 Hz, 2H, P−C$_6H_5$), 7.43 (td, $^{3}J_{H-P}$ = 7.7 Hz, $^{3}J_{H-H}$ = 2.5 Hz, 2H, PC$_6H_5$), 5.89 (dd, $^{3}J_{P-H}$ = 14.8 Hz, $^{3}J_{H-H}$ = 9.4 Hz, 1H, C*H*CH(PPh$_2$)Ar), 4.49 (dd, $^{2}J_{P-H}$ = 15.6 Hz, $^{3}J_{H-H}$ = 9.4 Hz, 1H, CHC*H*(PPh$_2$)Ar), 3.30 (s, 3H, COOCH_3), 3.25 (s), 2.76 (s), 2.73 (s, 3H, COOCH_3). ^{13}C NMR (126 MHz, $CDCl_3$): δ 166.89 (s, 1C, Ar, HC═CHN), 166.17 (d, $^{3}J_{P-C}$ = 12.0 Hz, 1C, C═O), 161.97 (d, $^{3}J_{P-C}$ = 8.1 Hz, 1C, C═O), 145.40 (s), 136.54 (s), 136.29 (d, $^{2}J_{P-C}$ = 11.3 Hz, 1C, Ar, N═*C*C(H)P), 133.44 (s), 133.10 (d, J_{P-C} = 2.8 Hz), 132.74 (d, J_{P-C} = 2.9 Hz), 132.61 (d, $^{1}J_{P-C}$ = 10.5 Hz, 1C, Ar, PC_6H_5), 129.93 (s), 129.71 (d, $^{1}J_{P-C}$ = 11.4 Hz, 1C, Ar, PC_6H_5), 128.62 (d, J_{P-C} = 12.1 Hz), 126.71 (d, J_{P-C} = 10.6 Hz), 125.04 (d, J_{P-C} = 53.6 Hz), 123.27 (s), 122.60 (d, J_{P-C} = 56.0 Hz), 53.22 (s, 1C, COOCH$_3$), 53.17 (d, $^{2}J_{P-C}$ = 5.3 Hz, 1C, CHCH(PPh$_2$)Ar), 52.71 (s, 1C, COOCH$_3$), 47.08 (d, $^{1}J_{P-C}$ = 30.4 Hz, 1C, CHCH(PPh$_2$)Ar), 30.93 (s), 29.69 (s). $^{31}P\{^{1}H\}$ NMR (202 MHz, $CDCl_3$): δ 52.13 (s). HRMS (+ESI). Calcd for $C_{27}H_{25}Cl_2NO_4PPd$ [(M + H)$^+$]: *m*/*z* 635.9937. Found: *m*/*z* 635.9931. Anal. Calcd for $C_{27}H_{24}Cl_2NO_4PPd$: C, 51.09; H, 3.81; N, 2.21. Found: C, 48.51; H, 3.61; N, 2.03.

*(R)-κ^2-P,N-[Dimethyl 2-(diphenylphosphaneyl)(isoquinolin-1-ylmethyl)malonate]dichloroplatinum(II) [(R)-**10**].* Yield: 67%, brown solid. $[\alpha]^{25}_{D}$ = −43 (*c* 0.5, CH_2Cl_2). ^{1}H NMR (500 MHz, $CDCl_3$): δ 10.03 (d, $^{3}J_{H-H}$ = 6.7 Hz, 1H, Ar*H*, HC═C*H*N), 8.30 (d, $^{3}J_{H-H}$ = 8.5 Hz, 1H, Ar*H*), 8.08−7.94 (m, 5H, Ar*H*), 7.93 (s, Ar*H*), 7.91 (s, 1H, Ar*H*), 7.90 (s, 1H, Ar*H*), 7.73 (m, 1H, Ar*H*), 7.69 (d, $^{3}J_{H-H}$ = 6.8 Hz, 1H, Ar*H*), 7.57 (m, 2H, Ar*H*), 7.53−7.41 (m, 6H, Ar*H*), 5.83 (dd, $^{3}J_{P-H}$ = 12.3 Hz, $^{3}J_{H-H}$ = 9.9 Hz, 1H, C*H*CH(PPh$_2$)Ar), 4.52 (dd, $^{2}J_{P-H}$ = 14.7 Hz, $^{3}J_{H-H}$ = 9.9 Hz, 1H, CHC*H*(PPh$_2$)Ar), 3.30 (s), 3.27 (s, 3H, COOCH_3), 2.74 (s), 2.69 (s, 3H, COOCH_3). ^{13}C NMR (126 MHz, $CDCl_3$): δ 166.98 (s, 1C, Ar, HC═CHN), 166.34 (d, $^{3}J_{P-C}$ = 12.2 Hz, 1C, C═O), 162.84 (d, $^{3}J_{P-C}$ = 5.7 Hz, 1C, C═O), 144.38 (s), 141.96 (s), 139.29 (s), 136.26 (d, $^{2}J_{P-C}$ = 11.7 Hz, 1C, Ar, N═CC(H)P), 135.95 (s), 133.18 (s), 132.94 (s), 132.66 (d, $^{1}J_{P-C}$ = 10.9 Hz, 1C, Ar, PC_6H_5), 132.45 (s), 130.16 (s), 129.50 (d, $^{1}J_{P-C}$ = 11.5 Hz, 1C, Ar, PC_6H_5), 128.51 (d, J_{P-C} = 12.4 Hz), 127.56 (d, J_{P-C} = 48.2 Hz), 126.99 (d, J_{P-C} = 8.7 Hz), 124.60 (d, J_{P-C} = 62.1 Hz), 123.34 (s), 120.84 (d, J_{P-C} = 63.8 Hz), 53.14 (s, 1C, COOCH$_3$), 52.56 (s, 1C, COOCH$_3$), 52.12 (d, $^{2}J_{P-C}$ = 4.3 Hz, 1C, *C*HCH(PPh$_2$)Ar), 46.23 (d, $^{1}J_{P-C}$ = 37.1 Hz, 1C, CHCH(PPh$_2$)Ar), 33.82 (s), 31.93 (s), 29.70 (s), 29.36 (s), 22.69 (s), 14.12 (s). $^{31}P\{^{1}H\}$ NMR (202 MHz, $CDCl_3$): δ 28.71 (s), 28.72

https://dx.doi.org/10.1021/acs.inorgchem.9b03549
Inorg. Chem. XXXX, XXX, XXX−XXX

(d, $^1J_{Pt-P}$ = 3826.9 Hz). HRMS (+ESI). Calcd for $C_{27}H_{25}Cl_2NO_4PPt$ [(M + H)$^+$]: m/z 723.0546. Found: m/z 723.0544. Anal. Calcd for $C_{27}H_{24}Cl_2NO_4PPt$: C, 44.83; H, 3.34; N, 1.94. Found: C, 44.67; H, 3.45; N, 2.10.

General Procedure for the Synthesis of P,N Rhodium and Iridium 1,5-Cyclooctadiene Tetrafluoroborate Complexes (13 and 14). [M(COD)Cl]$_2$ (0.04 mmol, 0.5 equiv) was dissolved in 5.0 mL of degassed DCM and stirred under nitrogen. $AgBF_4$ (0.08 mmol, 1.0 equiv) was dissolved in degassed methanol, and this was added to the DCM solution. This mixture was stirred at RT in the dark for 3 h. The resulting M$^+$(COD)$^-$BF$_4$ complex was filtered through a short Celite plug under nitrogen and immediately added to the DCM solution of P,N ligand **8** (0.08 mmol, 1.0 equiv; obtained in the aforementioned way) at −80 °C, stirred for 1 h under nitrogen, and allowed to reach RT. The formed (P,N)M$^+$(COD)$^-$BF$_4$ complex was filtered through a short Celite plug under Schlenk conditions, and the solvent was removed by vacuum.

*[κ^2-P,N-[Dimethyl 2-(diphenylphosphanyl)(isoquinolin-1-ylmethyl)malonate]][1,2,5,6-η-(1Z,5Z)-cycloocta-1,5-diene]-rhodium(I) Tetrafluoroborate (**13**).* Yield: crude brown solid. ^{1}H NMR (500 MHz, $CDCl_3$): δ 8.18 (d, $^3J_{H-H}$ = 8.7 Hz, 1H, Ar*H*), 8.07 (d, $^3J_{H-H}$ = 6.5 Hz, 1H, Ar*H*), 7.96 (t, $^3J_{H-H}$ = 9.1 Hz, 1H, Ar*H*), 7.89 (d, $^3J_{H-H}$ = 6.4 Hz, 1H, Ar*H*), 7.86 (d, $^3J_{H-H}$ = 8.3 Hz, 1H, Ar*H*), 7.77 (d, $^3J_{H-H}$ = 7.3 Hz, 1H, Ar*H*), 7.74−7.69 (m, 3H, Ar*H*), 7.68−7.63 (m, 1H, Ar*H*), 7.55−7.49 (m, 1H, Ar*H*), 7.48−7.38 (m, 5H, Ar*H*), 7.33−7.27 (m, 3H, Ar*H*), 5.88 (dd, $^3J_{P-H}$ = 13.2 Hz, $^3J_{H-H}$ = 8.1 Hz, 1H, C*H*CH(PPh$_2$)Ar), 5.67 (dd, $^3J_{H-H}$ = 15.1 Hz, $^2J_{Rh-H}$ = 1.4 Hz, 2H, COD *H*C = CH), 4.65 (dd, $^2J_{P-H}$ = 15.0 Hz, $^3J_{H-H}$ = 8.1 Hz, 1H, CHC*H*(PPh$_2$)Ar), 4.38 (d, $^3J_{H-H}$ = 55.1 Hz, $^2J_{Rh-H}$= 5.5 Hz, 2H, COD *H*C=CH), 3.70−3.60 (m), 3.46 (s, 3H, COOC*H*$_3$), 3.24−3.14 (m, 1H), 2.81 (s, 3H, COOC*H*$_3$), 2.74−2.53 (m, 2H, COD CH$_2$), 2.37 (m, 3H, COD C*H*$_2$), 2.10−1.99 (m, 2H, COD C*H*$_2$). ^{13}C NMR (126 MHz, $CDCl_3$): δ 167.26 (s, 1C, Ar, HC=*C*HN), 166.16 (d, $^3J_{P-C}$ = 9.4 Hz, 1C, *C*=O), 162.56 (d, $^3J_{P-C}$ = 9.3 Hz, 1C, *C*=O), 142.02 (s), 136.68 (s), 133.84−133.40 (m), 133.55 (d, $^2J_{P-C}$ = 10.8 Hz, 1C, Ar, N=C*C*(H)P), 133.16 (d, $^1J_{P-C}$ = 10.8 Hz, 1C, Ar, P*C*$_6$H$_5$) 132.51 (d, J_{P-C} = 2.4 Hz), 132.33 (d, J_{P-C} = 2.1 Hz), 130.07 (s), 129.63 (dd, $^2J_{Rh-C}$ = 20.9 Hz, $^1J_{P-C}$ = 10.3 Hz, 1C, Ar, P*C*$_6$H$_5$), 128.01 (s), 128.00 (s), 127.68 (s), 127.09 (s), 127.02 (s), 126.97 (s), 124.62 (d, J_{P-C} = 2.2 Hz), 124.45 (s), 124.32 (d, J_{P-C} = 2.7 Hz), 114.05 (s), 109.30−108.82 (m, 1C, COD, HC=CH), 107.50 (d, J = 7.8 Hz), 106.60−106.16 (m, 1C, COD, HC=CH), 79.44 (dd, $^2J_{P-C}$ = 10.8 Hz, $^1J_{Rh-C}$ = 4.9 Hz, 1C, COD, HC=CH), 78.07 (s), 76.47−76.24 (m, 1C, COD, HC=CH), 55.89 (d, $^2J_{P-C}$ = 8.4 Hz, 1C, *C*HCH(PPh$_2$)Ar), 53.46 (s, 1C, COOCH$_3$), 52.85 (s, 1C, COOCH$_3$), 47.75 (s), 47.59 (d, $^1J_{P-C}$ = 25.2 Hz, 1C, CHCH(PPh$_2$)-Ar), 35.55 (s), 33.81 (s), 31.91 (s), 30.88 (s), 29.34 (s), 29.14 (s), 28.97 (s), 26.03 (s), 22.67 (s), 18.36 (s), 14.10 (s), 9.13 (s), 1.00 (s). ^{19}F NMR (376 MHz, $CDCl_3$): δ −153.06 (s). ^{31}P{^{1}H} NMR (202 MHz, $CDCl_3$): δ 49.69 (d, $^1J_{Rh-P}$ = 156.2 Hz). HRMS (+ESI). Calcd for $C_{35}H_{37}NO_4PRh$ [(M + H − BF$_4^-$)$^+$]: m/z 669.1515. Found: m/z 669.1519.

*[κ^2-P,N-Dimethyl 2-(diphenylphosphaneyl)(isoquinolin-1-ylmethyl)malonate][1,2,5,6-η-(1Z,5Z)-cycloocta-1,5-diene]iridium-(I) Tetrafluoroborate (**14**).* Yield: crude dark-red solid. ^{1}H NMR (500 MHz, $CDCl_3$): δ 8.49 (d, $^3J_{H-H}$ = 6.5 Hz, 1H, Ar*H*), 8.20 (d, $^3J_{H-H}$ = 8.7 Hz, 1H, Ar*H*), 8.08 (d, $^3J_{H-H}$ = 6.4 Hz, 1H, Ar*H*), 7.93 (d, $^3J_{H-H}$ = 8.1 Hz, 1H, Ar*H*), 7.83−7.79 (m, 2H, Ar*H*), 7.72−7.61 (m, 4H, Ar*H*), 7.53 (d, $^3J_{H-H}$ = 3.9 Hz, 2H, Ar*H*), 7.50−7.43 (m, 4H, Ar*H*), 7.36 (d, $^3J_{H-H}$ = 5.2 Hz, 3H, Ar*H*), 7.16 (s, Ar*H*), 6.97 (d, $^3J_{H-H}$ = 9.2 Hz, 1H, Ar*H*), 6.09 (dd, $^3J_{P-H}$ = 12.2 Hz, $^3J_{H-H}$ = 9.05 Hz, 1H, C*H*CH(PPh$_2$)Ar), 5.62 (s, 1H, COD *H*C=CH), 5.36 (s, 1H, COD *H*C=CH), 4.56 (dd, $^2J_{P-H}$ = 14.1 Hz, $^3J_{H-H}$ = 9.05 Hz, 1H, CHC*H*(PPh$_2$)Ar), 4.20 (s, 1H, COD *H*C=CH), 3.82 (s, 1H, COD *H*C=CH), 3.42 (s), 3.40 (s, 3H, COOC*H*$_3$), 3.19−3.10 (m), 2.73 (s, 3H, COOC*H*$_3$), 2.58 (s, 4H, COD C*H*$_2$), 2.32−2.16 (m, 2H, COD C*H*$_2$), 1.82−1.65 (m, 2H, COD C*H*$_2$). ^{13}C NMR (126 MHz, $CDCl_3$): δ 167.03 (s, 1C, Ar, HC=*C*HN), 166.09 (d, $^3J_{P-C}$ = 10.3 Hz, 1C, *C*=O), 165.17 (d, $^3J_{P-C}$ = 7.4 Hz, 1C, *C*=O), 164.54 (s), 142.34 (s), 136.85 (s), 134.22−133.81 (m), 133.62 (d, $^2J_{P-C}$ = 10.6 Hz, 1C, Ar, N=C*C*(H)P), 132.72 (d, $^2J_{P-C}$ = 19.0 Hz, 1C, Ar, P*C*$_6$H$_5$), 131.12 (d, J_{P-C} = 9.0 Hz), 130.54 (s), 129.86 (d, $^2J_{P-C}$ = 10.7 Hz, 1C, Ar, P*C*$_6$H$_5$), 129.50 (d, J_{P-C} = 10.5 Hz), 129.01 (d, J_{P-C} = 9.9 Hz), 128.15 (s), 127.62 (s), 127.49 (s), 127.18−126.79 (m), 125.19 (s), 122.49 (d, J_{P-C} = 46.8 Hz), 99.76 (s), 97.35 (d, $^2J_{P-C}$ = 7.7 Hz, 1C, COD, HC=CH), 96.87 (d, $^2J_{P-C}$ = 8.9 Hz, 1C, COD, HC=CH), 65.79 (d, $^2J_{P-C}$ = 10.4 Hz, 1C, COD, HC=CH), 63.06 (d, $^2J_{P-C}$ = 13.8 Hz 1C, COD, HC=CH), 55.28 (d, $^2J_{P-C}$ = 6.8 Hz, 1C, *C*HCH(PPh$_2$)Ar), 53.43 (s, 1C, COOCH$_3$), 52.86 (s, 1C, COOCH$_3$), 49.59 (s), 48.22 (d, $^1J_{P-C}$ = 30.3 Hz, 1C, CH*C*H(PPh$_2$)-Ar), 47.73 (s), 43.77 (d, J = 8.6 Hz), 36.80 (s), 32.60 (s), 31.91 (s), 29.68 (s), 29.34 (s), 28.94 (s), 25.75 (s), 25.14 (s), 23.24 (d, J = 4.3 Hz), 23.04 (s), 22.68 (s), 14.10 (s), 9.13 (s). ^{19}F NMR (376 MHz, $CDCl_3$): δ −153.26 (s). ^{31}P{^{1}H} NMR (202 MHz, $CDCl_3$): δ 41.49 (s). HRMS (+ESI). Calcd for $C_{35}H_{37}NO_4PIr$ [(M + H − BF$_4^-$)$^+$]: m/z 759.2090. Found: m/z 759.2097.

Preparation of [(*R*)-κ^2-*C*^{2},*N*-1-[1-(Dimethylamino)ethyl]-naphthyl][(*R*)-κ^2-*P*,*N*-dimethyl 2-(diphenylphosphaneyl)-(isoquinolin-1-ylmethyl)malonate]palladium(II) Perchlorate [(*R*,*R*)-22]. Diphenylphosphine (0.08 mmol, 0.015 g, 1.0 equiv) was weighed into a Schlenk flask under positive nitrogen flow, and 3.0 mL of the previously degassed DCM was added. The malonate substrate **5a** (0.08 mmol, 0.022 g, 1.0 equiv) and (*S*)-**2** catalyst (0.004 mmol, 0.0025 g, 0.05 equiv) were added to the solution, and then the mixture was cooled to −80 °C. When the required temperature was reached, TEA (0.08 mmol, 0.009 g, 1.0 equiv) was added dropwise to the reaction mixture. After completion of the reaction, the (*R*)-**1** complex (0.08 mmol, 0.042 g, 1.0 equiv) was added, and the mixture was allowed to warm to RT. The solution was washed with water and brine, dried, and filtered through a short Celite plug, and then the solvent was evaporated. The crude complex was recrystallized from DCM with diethyl ether to afford diastereomerically pure crystals. (*R*,*R*)-**22** is a bright-yellow solid. Yield: 33%. $[\alpha]^{25}_D$ = −247 (*c* 2.0, CH_2Cl_2). ^{1}H NMR (500 MHz, $CDCl_3$): δ 8.72 (d, $^3J_{H-H}$ = 6.1 Hz, 1H, Ar*H*, HC=C*H*N), 8.32 (d, $^3J_{H-H}$ = 8.6 Hz, 1H, Ar*H*), 8.25 (d, $^3J_{H-H}$ = 6.1 Hz, 1H, Ar*H*), 7.99 (d, $^3J_{H-H}$ = 8.2 Hz, 1H, Ar*H*), 7.89−7.76 (m, 5H, Ar*H*), 7.74 (d, $^3J_{H-H}$ = 8.1 Hz, 1H, Ar*H*), 7.58−7.47 (m, 5H, Ar*H*), 7.47−7.40 (m, 3H, Ar*H*), 7.30 (t, $^3J_{H-H}$ = 6.9 Hz, 2H, Ar*H*), 7.20 (d, $^3J_{H-H}$ = 8.4 Hz, 1H, Ar*H*), 6.97−6.91 (m, 1H, Ar*H*), 5.91 (dd, $^3J_{H-P}$ = 13.7 Hz, $^3J_{H-H}$ = 8.6 Hz, 1H, C*H*CH(PPh$_2$)Ar), 4.74−4.60 (m, 2H, NC*H*CH$_3$, CHC*H*(PPh$_2$)Ar), 3.31 (s, 3H, COOC*H*$_3$), 3.28 (s), 3.19 (s), 3.13 (d, $^4J_{P-H}$ = 3.0 Hz, 3H, NC*H*$_3$), 3.09 (s, 3H, NC*H*$_3$), 2.85 (s, 3H, COOC*H*$_3$), 2.22 (d, $^3J_{H-H}$ = 6.2 Hz, 3H, NCHC*H*$_3$), 1.29 (s), 1.26 (s). ^{13}C NMR (126 MHz, $CDCl_3$): δ 166.60 (s, 1C, Ar, HC=*C*H−N), 165.95 (d, $^3J_{P-C}$ = 11.3 Hz, 1C, *C*=O), 158.91 (d, $^3J_{P-C}$ = 5.4 Hz, 1C, *C*=O), 150.18 (s), 146.55 (s), 142.29 (s), 137.27 (d, $^2J_{P-C}$ = 12.6 Hz, Ar, N=C*C*(H)P), 137.02 (s), 135.44 (d, $^1J_{P-C}$ = 12.0 Hz, Ar, P*C*$_6$H$_5$), 133.17 (s), 133.07 (s), 132.96 (t, 1C, J_{P-C} = 2.8 Hz, Ar), 131.81 (s), 130.06 (s), 129.96 (d, J_{P-C} = 4.5 Hz, 1C, Ar), 129.01 (d, $^1J_{P-C}$ = 11.2 Hz, Ar, P*C*$_6$H$_5$), 128.91 (d, J_{P-C} = 3.9 Hz), 128.37 (s), 127.11 (d, J_{P-C} = 6.0 Hz), 126.66 (d, J_{P-C} = 7.2 Hz), 126.30 (s), 125.39 (s), 125.18 (s), 124.80 (s), 123.27 (s), 123.17 (s), 122.82 (s), 74.33 (d, $^3J_{P-C}$ = 2.8 Hz, 1C, NCH$_3$), 55.02 (d, $^2J_{P-C}$ = 9.4 Hz, 1C, CHCH(PPh$_2$)Ar), 53.23 (s, 1C, COOCH$_3$), 52.89 (s, 1C, COOCH$_3$), 52.09 (d, $^3J_{P-C}$ = 2.4 Hz, 1C, NCH$_3$), 47.29 (s, 1C, NCHCH$_3$), 46.08 (d, $^1J_{P-C}$ = 32.3 Hz, 1C, CHCH(PPh$_2$)Ar), 29.69 (s), 24.51 (s, 1C, NCHCH$_3$). ^{31}P{^{1}H} NMR (202 MHz, $CDCl_3$): δ 57.75 (s), 54.85 (s). HRMS (+ESI). Calcd for $C_{41}H_{41}ClN_2O_8PPd$ [(M + H)$^+$]: m/z 861.1324. Found: m/z 861.1301.

■ ASSOCIATED CONTENT

Supporting Information

The Supporting Information is available free of charge at https://pubs.acs.org/doi/10.1021/acs.inorgchem.9b03549.

General information, experimental methods, NMR spectra, HPLC chromatograms, coordination study, NBO analysis, *XYZ* coordinates for the optimized geometries, and X-ray crystallographic data (PDF)

https://dx.doi.org/10.1021/acs.inorgchem.9b03549
Inorg. Chem. XXXX, XXX, XXX−XXX

Accession Codes

CCDC 1968108, 1968110, and1968111 contain the supplementary crystallographic data for this paper. These data can be obtained free of charge via www.ccdc.cam.ac.uk/data_request/cif, or by emailing data_request@ccdc.cam.ac.uk, or by contacting The Cambridge Crystallographic Data Centre, 12 Union Road, Cambridge CB2 1EZ, UK; fax: +44 1223 336033.

AUTHOR INFORMATION

Corresponding Authors

Sumod A. Pullarkat − *Division of Chemistry and Biological Chemistry, School of Physical and Mathematical Sciences, Nanyang Technological University, Singapore 637371 Singapore;* orcid.org/0000-0002-4150-2408; Email: sumod@ntu.edu.sg

Pak-Hing Leung − *Division of Chemistry and Biological Chemistry, School of Physical and Mathematical Sciences, Nanyang Technological University, Singapore 637371 Singapore;* orcid.org/0000-0003-3588-1664; Email: pakhing@ntu.edu.sg

Authors

Dávid Katona − *Division of Chemistry and Biological Chemistry, School of Physical and Mathematical Sciences, Nanyang Technological University, Singapore 637371 Singapore;* orcid.org/0000-0001-7109-3716

Yunpeng Lu − *Division of Chemistry and Biological Chemistry, School of Physical and Mathematical Sciences, Nanyang Technological University, Singapore 637371 Singapore;* orcid.org/0000-0003-2493-7853

Yongxin Li − *Division of Chemistry and Biological Chemistry, School of Physical and Mathematical Sciences, Nanyang Technological University, Singapore 637371 Singapore;* orcid.org/0000-0002-7860-3237

Complete contact information is available at: https://pubs.acs.org/10.1021/acs.inorgchem.9b03549

Notes

The authors declare no competing financial interest.

ACKNOWLEDGMENTS

We thank Nanyang Technological University for enabling and supporting our research [Grants M4080454 (NTU) and 2017-T1-001-175-02 (MOE)] and for a SINGA scholarship supporting D.K. in his studies. We also thank Li Xi-Rui for providing the P,C analogue of our complexes for the coordination study.

REFERENCES

(1) (a) Evans, D. A.; Miller, S. J.; Lectka, T.; von Matt, P. Chiral Bis(oxazoline)copper(II) Complexes as Lewis Acid Catalysts for the Enantioselective Diels-Alder Reaction. *J. Am. Chem. Soc.* **1999**, *121* (33), 7559−7573. (b) Thorhauge, J.; Roberson, M.; Hazell, R. G.; Jørgensen, K. A. On the Intermediates in Chiral Bis(oxazoline)-copper(II)-Catalyzed Enantioselective Reactions—Experimental and Theoretical Investigations. *Chem. - Eur. J.* **2002**, *8* (8), 1888−1898. (c) Bronger, R. P. J.; Bermon, J. P.; Herwig, J.; Kamer, P. C. J.; van Leeuwen, P. W. N. M. Phenoxaphosphino-Modified Xantphos-Type Ligands in the Rhodium-Catalysed Hydroformylation of Internal and Terminal Alkenes. *Adv. Synth. Catal.* **2004**, *346* (7), 789−799. (d) van der Vlugt, J. I.; Hewat, A. C.; Neto, S.; Sablong, R.; Mills, A. M.; Lutz, M.; Spek, A. L.; Müller, C.; Vogt, D. Sterically Demanding Diphosphonite Ligands − Synthesis and Application in Nickel-Catalyzed Isomerization of 2-Methyl-3-Butenenitrile. *Adv. Synth. Catal.* **2004**, *346* (8), 993−1003. (e) Casey, C. P.; Whiteker, G. T. The Natural Bite Angle of Chelating Diphosphines. *Isr. J. Chem.* **1990**, *30* (4), 299−304. (f) Birkholz, M.-N.; Freixa, Z.; van Leeuwen, P. W. N. M. Bite angle effects of diphosphines in C−C and C−X bond forming cross coupling reactions. *Chem. Soc. Rev.* **2009**, *38* (4), 1099−1118.

(2) (a) Vineyard, B. D.; Knowles, W. S.; Sabacky, M. J.; Bachman, G. L.; Weinkauff, D. J. Asymmetric hydrogenation. Rhodium chiral bisphosphine catalyst. *J. Am. Chem. Soc.* **1977**, *99* (18), 5946−5952. (b) Noyori, R.; Ohkuma, T.; Kitamura, M.; Takaya, H.; Sayo, N.; Kumobayashi, H.; Akutagawa, S. Asymmetric hydrogenation of. beta.-keto carboxylic esters. A practical, purely chemical access to. beta.-hydroxy esters in high enantiomeric purity. *J. Am. Chem. Soc.* **1987**, *109* (19), 5856−5858. (c) Halpern, J. Mechanism and Stereoselectivity of Asymmetric Hydrogenation. *Science* **1982**, *217* (4558), 401−407. (d) Casey, C. P.; Whiteker, G. T.; Melville, M. G.; Petrovich, L. M.; Gavney, J. A.; Powell, D. R. Diphosphines with natural bite angles near 120.degree. increase selectivity for n-aldehyde formation in rhodium-catalyzed hydroformylation. *J. Am. Chem. Soc.* **1992**, *114* (14), 5535−5543. (e) Nettekoven, U.; Widhalm, M.; Kalchhauser, H.; Kamer, P. C. J.; van Leeuwen, P. W. N. M.; Lutz, M.; Spek, A. L. Steric and Electronic Ligand Perturbations in Catalysis: Asymmetric Allylic Substitution Reactions Using C2-Symmetrical Phosphorus-Chiral (Bi)ferrocenyl Donors. *J. Org. Chem.* **2001**, *66* (3), 759−770. (f) Imamoto, T.; Watanabe, J.; Wada, Y.; Masuda, H.; Yamada, H.; Tsuruta, H.; Matsukawa, S.; Yamaguchi, K. P-Chiral Bis(trialkylphosphine) Ligands and Their Use in Highly Enantioselective Hydrogenation Reactions. *J. Am. Chem. Soc.* **1998**, *120* (7), 1635−1636. (g) Imamoto, T.; Itoh, T.; Yamanoi, Y.; Narui, R.; Yoshida, K. Highly enantioselective hydrosilylation of simple ketones catalyzed by rhodium complexes of P-chiral diphosphine ligands bearing tert-butylmethylphosphino groups. *Tetrahedron: Asymmetry* **2006**, *17* (4), 560−565. (h) Dutartre, M.; Bayardon, J.; Jugé, S. Applications and stereoselective syntheses of P-chirogenic phosphorus compounds. *Chem. Soc. Rev.* **2016**, *45* (20), 5771−5794.

(3) (a) Togni, A. Planar-Chiral Ferrocenes: Synthetic Methods and Applications. *Angew. Chem., Int. Ed. Engl.* **1996**, *35* (13−14), 1475−1477. (b) Guiry, P. J.; Saunders, C. P. The Development of Bidentate P, N Ligands for Asymmetric Catalysis. *Adv. Synth. Catal.* **2004**, *346* (5), 497−537. (c) Rokade, B. V.; Guiry, P. J. Axially Chiral P, N-Ligands: Some Recent Twists and Turns. *ACS Catal.* **2018**, *8* (1), 624−643. (d) Mothes, E.; Sentets, S.; Luquin, M. A.; Mathieu, R.; Lugan, N.; Lavigne, G. New Insight into the Reactivity of Pyridine-Functionalized Phosphine Complexes of Ruthenium(II) with Respect to Olefin Metathesis and Transfer Hydrogenation. *Organometallics* **2008**, *27* (6), 1193−1206. (e) Yang, H.; Gao, H.; Angelici, R. J. Hydrogenation of Arenes under Mild Conditions Using Rhodium Pyridylphosphine and Bipyridyl Complexes Tethered to a Silica-Supported Palladium Heterogeneous Catalyst. *Organometallics* **2000**, *19* (4), 622−629.

(4) (a) Wang, Y.; Guo, H.; Ding, K. Synthesis of novel N, P chiral ligands for palladium-catalyzed asymmetric allylations: the effect of binaphthyl backbone on the enantioselectivity. *Tetrahedron: Asymmetry* **2000**, *11* (20), 4153−4162. (b) Brown, J. M.; Hulmes, D. I.; Guiry, P. J. Mechanistic and synthetic studies in catalytic allylic alkylation with palladium complexes of 1-(2-diphenylphosphino-1-naphthyl)isoquinoline. *Tetrahedron* **1994**, *50* (15), 4493−4506.

(5) (a) Cahard, D.; Gaillard, S.; Renaud, J.-L. Asymmetric isomerization of allylic alcohols. *Tetrahedron Lett.* **2015**, *56* (45), 6159−6169. (b) Mantilli, L.; Gérard, D.; Torche, S.; Besnard, C.; Mazet, C. Iridium-Catalyzed Asymmetric Isomerization of Primary Allylic Alcohols. *Angew. Chem., Int. Ed.* **2009**, *48* (28), 5143−5147.

(6) Li, J.-Q.; Liu, J.; Krajangsri, S.; Chumnanvej, N.; Singh, T.; Andersson, P. G. Asymmetric Hydrogenation of Allylic Alcohols Using Ir−N, P-Complexes. *ACS Catal.* **2016**, *6* (12), 8342−8349.

(7) (a) Doucet, H.; Fernandez, E.; Layzell, T. P.; Brown, J. M. The Scope of Catalytic Asymmetric Hydroboration/Oxidation with Rhodium Complexes of 1,1′-(2-Diarylphosphino-1-naphthyl)-isoquinolines. *Chem. - Eur. J.* **1999**, *5* (4), 1320−1330. (b) Maeda,

K.; Brown, J. M. Efficient kinetic resolution in hydroboration of 1,2-dihydronaphthalenes. *Chem. Commun. (Cambridge, U. K.)* **2002**, No. 4, 310−311. (c) Kwong, F. Y.; Yang, Q.; Mak, T. C. W.; Chan, A. S. C.; Chan, K. S. A New Atropisomeric P, N Ligand for Rhodium-Catalyzed Asymmetric Hydroboration. *J. Org. Chem.* **2002**, *67* (9), 2769−2777.

(8) Guiry, P. J.; Hennessy, A. J.; Cahill, J. P. The asymmetric Heck reaction: recent developments and applications of new palladium diphenylphosphinopyrrolidine complexes. *Top. Catal.* **1997**, *4* (3), 311−326.

(9) (a) Miyashita, A.; Yasuda, A.; Takaya, H.; Toriumi, K.; Ito, T.; Souchi, T.; Noyori, R. Synthesis of 2,2′-bis(diphenylphosphino)-1,1′-binaphthyl (BINAP), an atropisomeric chiral bis(triaryl)phosphine, and its use in the rhodium(I)-catalyzed asymmetric hydrogenation of. alpha.-(acylamino)acrylic acids. *J. Am. Chem. Soc.* **1980**, *102* (27), 7932−7934. (b) Miyashita, A.; Takaya, H.; Souchi, T.; Noyori, R. 2, 2′-bis(diphenylphosphino)-1, 1′-binaphthyl(binap): A new atropisomeric bis(triaryl)phosphine. synthesis and its use in the rh(l)-catalyzed asymmetric hydrogenation of α-(acylamino)acrylic acids. *Tetrahedron* **1984**, *40* (8), 1245−1253. (c) Akutagawa, S. Asymmetric synthesis by metal BINAP catalysts. *Appl. Catal., A* **1995**, *128* (2), 171−207.

(10) (a) Alcock, N. W.; Brown, J. M.; Hulmes, D. I. Synthesis and resolution of 1-(2-diphenylphosphino-1-naphthyl)isoquinoline; a P—N chelating ligand for asymmetric catalysis. *Tetrahedron: Asymmetry* **1993**, *4* (4), 743−756. (b) Fernández, E.; Guiry, P. J.; Connole, K. P. T.; Brown, J. M. Quinap and Congeners: Atropos PN ligands for Asymmetric Catalysis. *J. Org. Chem.* **2014**, *79* (12), 5391−5400.

(11) (a) Huang, Y.; Pullarkat, S. A.; Li, Y.; Leung, P.-H. Palladacycle-Catalyzed Asymmetric Hydrophosphination of Enones for Synthesis of C*- and P*-Chiral Tertiary Phosphines. *Inorg. Chem.* **2012**, *51* (4), 2533−2540. (b) Allen, D. G.; McLaughlin, G. M.; Robertson, G. B.; Steffen, W. L.; Salem, G.; Wild, S. B. Resolutions with metal complexes. Preparation and resolution of (R, S)-methylphenyl(8-quinolyl)phosphine and its arsenic analog. Crystal and molecular structure of (+)589-[(R)-dimethyl(1-ethyl-.alpha.-naphthyl)aminato-C2, N][(S)-methylphenyl(8-quinolyl)phosphine]-palladium(II) hexafluorophosphate. *Inorg. Chem.* **1982**, *21* (3), 1007−1014. (c) Ding, Y.; Zhang, Y.; Li, Y.; Pullarkat, S. A.; Andrews, P.; Leung, P.-H. Synthesis of a Chiral Palladacycle and Its Application in Asymmetric Hydrophosphanation Reactions. *Eur. J. Inorg. Chem.* **2010**, *2010* (28), 4427−4437. (d) Chew, R. J.; Leung, P.-H. Our Odyssey with Functionalized Chiral Phosphines: From Optical Resolution to Asymmetric Synthesis to Catalysis. *Chem. Rec.* **2016**, *16* (1), 141−158. (e) Dunina, V. V.; Gorunova, O. N. Phosphapalladacycles: forms of existence and reactions. *Russ. Chem. Rev.* **2005**, *74* (10), 871−913. (f) Farina, V. High-Turnover Palladium Catalysts in Cross-Coupling and Heck Chemistry: A Critical Overview. *Adv. Synth. Catal.* **2004**, *346* (13−15), 1553−1582.

(12) (a) Liu, F.; Pullarkat, S. A.; Tan, K.-W.; Li, Y.; Leung, P.-H. Organoplatinum Complex Promoted the Asymmetric Endo Stereochemically Controlled Diels-Alder Reaction between 3-Diphenylphosphinofuran and Diphenylvinylphosphine. *Inorg. Chem.* **2009**, *48* (23), 11394−11398. (b) Yuan, M.; Pullarkat, S. A.; Yeong, C. H.; Li, Y.; Krishnan, D.; Leung, P.-H. Controllable synthesis of P-chiral 1,2- and 1,3-diphosphines via asymmetric Diels−Alder reactions involving functionalized allylic phosphines as dienophiles. *Dalton Trans.* **2009**, No. 19, 3668−3670.

(13) Pullarkat, S. A. Recent Progress in Palladium-Catalyzed Asymmetric Hydrophosphination. *Synthesis* **2016**, *48* (04), 493−503.

(14) (a) Ng, J. K.-P.; Tan, G.-K.; Vittal, J. J.; Leung, P.-H. Optical Resolution and the Study of Ligand Effects on the Ortho-Metalation Reaction of Resolved (±)-Diphenyl[1-(1-naphthyl)ethyl]phosphine and Its Arsenic Analogue. *Inorg. Chem.* **2003**, *42* (23), 7674−7682. (b) Ng, J. K. P.; Chen, S.; Tan, G. K.; Leung, P.-H. Conformational analyses of the five-membered palladacycles derived from 1-(1′-naphthyl)ethyldiphenylphosphine and its arsenic analogue. *Tetrahedron: Asymmetry* **2007**, *18* (10), 1163−1169.

(15) (a) Espinet, P.; Soulantica, K. Phosphine-pyridyl and related ligands in synthesis and catalysis. *Coord. Chem. Rev.* **1999**, *193*−*195*, 499−556. (b) Fanfoni, L.; Meduri, A.; Zangrando, E.; Castillon, S.; Felluga, F.; Milani, B. New Chiral P-N Ligands for the Regio- and Stereoselective Pd-Catalyzed Dimerization of Styrene. *Molecules* **2011**, *16* (2), 1804−1824.

(16) Bhat, V.; Wang, S.; Stoltz, B. M.; Virgil, S. C. Asymmetric Synthesis of QUINAP via Dynamic Kinetic Resolution. *J. Am. Chem. Soc.* **2013**, *135* (45), 16829−16832.

(17) Ramírez-López, P.; Ros, A.; Estepa, B.; Fernández, R.; Fiser, B.; Gómez-Bengoa, E.; Lassaletta, J. M. A Dynamic Kinetic C−P Cross−Coupling for the Asymmetric Synthesis of Axially Chiral P, N Ligands. *ACS Catal.* **2016**, *6* (6), 3955−3964.

(18) Giordano, C.; Minisci, F.; Vismara, E.; Levi, S. A general, selective, and convenient procedure of homolytic formylation of heteroaromatic bases. *J. Org. Chem.* **1986**, *51* (4), 536−537.

(19) Ganley, J. M.; Christensen, M.; Lam, Y.-h.; Peng, Z.; Angeles, A. R.; Yeung, C. S. Metal- and Acid-Free C−H Formylation of Nitrogen Heterocycles: Using Trioxane as an Aldehyde Equivalent Enabled by an Organic-Soluble Oxidant. *Org. Lett.* **2018**, *20* (18), 5752−5756.

(20) (a) Allinson, G.; Bushby, R. J.; Jesudason, M. V.; Paillaud, J.-L.; Taylor, N. The synthesis of singlet ground state derivatives of non-Kekulé polynuclear aromatics. *J. Chem. Soc., Perkin Trans. 2* **1997**, No. 2, 147−156. (b) Chen, H.; Luzy, J.-P.; Gresh, N.; Garbay, C. An Efficient and Enantioselective Synthesis of Suitably Protected β-[1-(4-Malonyl)naphthyl]-L-alanine and β-[1-(4-Malonylmethyl)naphthyl]-L-alanine: Novel Fluorescent and Non-Hydrolysable Phosphotyrosine Mimetics. *Eur. J. Org. Chem.* **2006**, *2006* (10), 2329−2335.

(21) (a) Li, X.-R.; Yang, X.-Y.; Li, Y.; Pullarkat, S. A.; Leung, P.-H. Efficient access to a designed phosphapalladacycle catalyst via enantioselective catalytic asymmetric hydrophosphination. *Dalton Trans.* **2017**, *46* (4), 1311−1316. (b) Yang, X.-Y.; Tay, W. S.; Li, Y.; Pullarkat, S. A.; Leung, P.-H. Versatile Syntheses of Optically Pure PCE Pincer Ligands: Facile Modifications of the Pendant Arms and Ligand Backbones. *Organometallics* **2015**, *34* (8), 1582−1588.

(22) Xu, C.; Jun Hao Kennard, G.; Hennersdorf, F.; Li, Y.; Pullarkat, S. A.; Leung, P.-H. Chiral Phosphapalladacycles as Efficient Catalysts for the Asymmetric Hydrophosphination of Substituted Methylidenemalonate Esters: Direct Access to Functionalized Tertiary Chiral Phosphines. *Organometallics* **2012**, *31* (8), 3022−3026.

(23) Jia, Y.-X.; Jonathan Chew, R.; Li, B.-B.; Zhu, P.; Li, Y.; Pullarkat, S. A.; Soon Tan, N.; Leung, P.-H. Palladacycle promoted base controlled regio- and enantioselective hydrophosphination of 2-pyridylacrylate/amide and the cytotoxicity of their gold complexes. *Dalton Trans.* **2015**, *44* (40), 17557−17564.

(24) Yang, X.-Y.; Jia, Y.-X.; Tay, W. S.; Li, Y.; Pullarkat, S. A.; Leung, P.-H. Mechanistic insights into the role of PC- and PCP-type palladium catalysts in asymmetric hydrophosphination of activated alkenes incorporating potential coordinating heteroatoms. *Dalton Trans.* **2016**, *45* (34), 13449−13455.

(25) (a) Jia, Y.-X.; Li, B.-B.; Li, Y.; Pullarkat, S. A.; Xu, K.; Hirao, H.; Leung, P.-H. Stereoelectronic and Catalytic Properties of Chiral Cyclometalated Phospha-palladium and -platinum Complexes. *Organometallics* **2014**, *33* (21), 6053−6058. (b) Pidcock, A.; Richards, R. E.; Venanzi, L. M. 195Pt−31P nuclear spin coupling constants and the nature of the trans-effect in platinum complexes. *J. Chem. Soc. A* **1966**, *0* (0), 1707−1710.

(26) Aydemir, M.; Meric, N.; Kayan, C.; Ok, F.; Baysal, A. Rhodium-catalyzed transfer hydrogenation with functionalized bis(phosphino)-amine ligands. *Inorg. Chim. Acta* **2013**, *398*, 1−10.

(27) Brown, T. H.; Green, P. J. Phosphorus-31 and rhodium-103 nuclear magnetic resonance spectra of some rhodium(I) and rhodium(III) phosphine complexes. *J. Am. Chem. Soc.* **1970**, *92* (8), 2359−2362.

(28) Flack, H. D.; Bernardinelli, G. The use of X-ray crystallography to determine absolute configuration. *Chirality* **2008**, *20* (5), 681−690.

(29) Nixon, J. F.; Pidcock, A. Phosphorus-31 Nuclear Magnetic Resonance Spectra of Coordination Compounds. In *Annual Report on*

https://dx.doi.org/10.1021/acs.inorgchem.9b03549
Inorg. Chem. XXXX, XXX, XXX−XXX

NMR Spectroscopy; Mooney, E. F., Ed.; Academic Press, 1969; Vol. 2, pp 345−422.
(30) Coe, B. J.; Glenwright, S. J. Trans-effects in octahedral transition metal complexes. *Coord. Chem. Rev.* **2000**, *203* (1), 5−80.
(31) Frisch, M. J.; Trucks, G. W.; Schlegel, H. B.; Scuseria, G. E.; Robb, M. A.; Cheeseman, J. R.; Scalmani, G.; Barone, V.; Petersson, G. A.; Nakatsuji, H.; Li, X.; Caricato, M.; Marenich, A. V.; Bloino, J.; Janesko, B. G.; Gomperts, R.; Mennucci, B.; Hratchian, H. P.; Ortiz, J. V.; Izmaylov, A. F.; Sonnenberg, J. L.; Williams; Ding, F.; Lipparini, F.; Egidi, F.; Goings, J.; Peng, B.; Petrone, A.; Henderson, T.; Ranasinghe, D.; Zakrzewski, V. G.; Gao, J.; Rega, N.; Zheng, G.; Liang, W.; Hada, M.; Ehara, M.; Toyota, K.; Fukuda, R.; Hasegawa, J.; Ishida, M.; Nakajima, T.; Honda, Y.; Kitao, O.; Nakai, H.; Vreven, T.; Throssell, K.; Montgomery, J. A., Jr.; Peralta, J. E.; Ogliaro, F.; Bearpark, M. J.; Heyd, J. J.; Brothers, E. N.; Kudin, K. N.; Staroverov, V. N.; Keith, T. A.; Kobayashi, R.; Normand, J.; Raghavachari, K.; Rendell, A. P.; Burant, J. C.; Iyengar, S. S.; Tomasi, J.; Cossi, M.; Millam, J. M.; Klene, M.; Adamo, C.; Cammi, R.; Ochterski, J. W.; Martin, R. L.; Morokuma, K.; Farkas, O.; Foresman, J. B.; Fox, D. J. *Gaussian 16*, revision C.01; Gaussian Inc.: Wallingford, CT, 2016.
(32) Reed, A. E.; Curtiss, L. A.; Weinhold, F. Intermolecular interactions from a natural bond orbital, donor-acceptor viewpoint. *Chem. Rev. (Washington, DC, U. S.)* **1988**, *88* (6), 899−926.
(33) (a) Becke, A. D. Density-functional thermochemistry. III. The role of exact exchange. *J. Chem. Phys.* **1993**, *98* (7), 5648−5652. (b) Lee, C.; Yang, W.; Parr, R. G. Development of the Colle-Salvetti correlation-energy formula into a functional of the electron density. *Phys. Rev. B: Condens. Matter Mater. Phys.* **1988**, *37* (2), 785−789. (c) Stephens, P. J.; Devlin, F. J.; Chabalowski, C. F.; Frisch, M. J. Ab Initio Calculation of Vibrational Absorption and Circular Dichroism Spectra Using Density Functional Force Fields. *J. Phys. Chem.* **1994**, *98* (45), 11623−11627. (d) Vosko, S. H.; Wilk, L.; Nusair, M. Accurate spin-dependent electron liquid correlation energies for local spin density calculations: a critical analysis. *Can. J. Phys.* **1980**, *58* (8), 1200−1211.
(34) (a) Dolg, M.; Wedig, U.; Stoll, H.; Preuss, H. Energy-adjusted abinitio pseudopotentials for the first row transition elements. *J. Chem. Phys.* **1987**, *86* (2), 866−872. (b) Hehre, W.; Radom, L.; Schleyer, P. V. R.; Pople, J. *Ab Initio Molecular Orbital Theory*; John Wiley & Sons: New York, 1986.
(35) Law, D. J.; Bigam, G.; Cavell, R. G. Preparation and properties of rhodium(I) and iridium(I) diolefin complexes of heterodifunctional phosphorus−imine chelating ligands and a related iminophosphine. 103Rh NMR parameters of the rhodium complexes obtained via indirect two-dimensional 31P, 103Rh{1H} NMR spectroscopy. *Can. J. Chem.* **1995**, *73* (5), 635−642.
(36) Moreton, S. NMR studies of some carbonyl complexes of iridium(I) and (III). *Inorg. Chim. Acta* **1992**, *202* (2), 225−230.

https://dx.doi.org/10.1021/acs.inorgchem.9b03549
Inorg. Chem. XXXX, XXX, XXX−XXX